In: AIAA SciTech Forum 2023, 23-27 January 2023, National Harbor, Maryland, USA
DOI:10.2514/6.2023-0840

Integrated Mission Performance Analysis of Novel Propulsion Systems: Analysis of a Fuel Cell Regional Aircraft Retrofit

Evangelia Pontika[1], Bahareh Zaghari[2], Tianzhi Zhou[3], Hossein Balaghi Enalou[4] and Panagiotis Laskaridis[5]
Cranfield University, Bedford, MK430AL, United Kingdom

This paper presents the development and application of an integrated, higher-fidelity framework developed within CHARM (the Cranfield Hybrid electric Aircraft Model) for the design, performance analysis and overall evaluation of novel electrified propulsion systems. The developed framework is used to model and analyze the performance characteristics of a Fuel Cell (FC) regional aircraft system in comparison with a conventional regional aircraft and a hydrogen gas turbine regional aircraft retrofit. The FC propulsion system and the hydrogen gas turbine are retrofitted to the same conventional aircraft platform. Physics-based aircraft performance calculations, propeller maps, gas turbine component maps, off-design cycle analysis, electric component maps, calculations for the electric power management and distribution, and a Proton-Exchange Membrane FC (PEMFC) configuration sized to cover the power requirements of a regional aircraft, are integrated within this framework to capture the performance and interaction of components, sub-systems and aircraft during any flight mission and conditions. The aircraft performance, the propulsion system performance characteristics and the emissions of the three technologies are calculated and discussed to understand the challenges and opportunities of using hydrogen-electric propulsion (FC). The effect of capturing the variable mission parameters and flight phases on the performance of the electric power system and FC is presented and compared against a lower fidelity modeling approach for the electric powertrain. The sensitivity of the FC propulsion system and its attributes to varying mission requirements (island-hopping, range, cruise altitude, ambient conditions), as well as the change in the consumed fuel, are demonstrated. This framework can be used to inform the decision-making for the design of electric components and thermal management systems (TMS), and the importance of capturing the trade-off between mass, efficiency and operational constraints in the design process is highlighted. Also, the off-design performance of the electric power system designs and FC is modeled to decide if the design is within acceptable limits under various conditions, and capture the effect of mission requirements and flight conditions on the energy consumption of the overall aircraft system. Finally, a parametric analysis addresses the effect of power density improvement with future technology on the energy per passenger and feasibility of the FC regional aircraft.

[1] Research Fellow in Propulsion Performance and Fleet Management, Centre for Propulsion and Thermal Power Engineering, AIAA member
[2] Lecturer in Propulsion Integration, Centre for Propulsion and Thermal Power Engineering, AIAA member
[3] PhD Candidate in Electric Propulsion Architectures, Centre for Propulsion and Thermal Power Engineering
[4] Research Fellow in Hybrid Electric Propulsion Architectures, Centre for Propulsion and Thermal Power Engineering
[5] Professor of Hybrid Electric Propulsion, Centre for Propulsion and Thermal Power Engineering, AIAA member

I. Nomenclature

AC	=	*aircraft*
β	=	propeller pitch angle
C_P	=	propeller power coefficient
C_T	=	propeller thrust coefficient
H_2	=	Hydrogen
J	=	*Advance Ratio*
LHV	=	*Lower Heating Value*
HHV	=	*Higher Heating Value*
MTOW	=	Maximum Take-off Weight
m_f	=	fuel mass
N	=	Shaft/Propeller/Motor rotational speed
OEW	=	Operating Empty Weight
TET	=	Turbine Entry Temperature

II. Introduction

A. Motivation

There has been an increasing international effort to reduce the carbon and non-carbon emissions of aviation with roadmaps to reduce by 55% aviation carbon emissions by 2030 and by 2050 to achieve zero net carbon emissions [1]. Apart from battery electrification concepts, hydrogen is one of the most promising cleaner alternatives to kerosene-fuelled propulsion for regional and commuter aircraft. Emerging hydrogen technologies include fuel cells (FCs), hydrogen gas turbines (GT), batteries and hybrid combinations of the above. Proton-Exchange Membrane Fuel Cells (PEMFC) become particularly attractive because they have higher efficiency than gas turbines, they eliminate CO_2 and NOx emissions, which may still be present in hydrogen combustion and among different types of Fuel Cells and batteries, they exhibit higher power density [2]. However, there are technological constraints that impose challenges, and the application of novel propulsion systems is dependent on the evolution of several technology factors, from the power densities of the fuel cells, thermal management system and electrical powertrains to hydrogen tank gravimetric efficiency and hydrogen tank volume.

B. State of the Art

1. Novel Propulsion Systems for Regional Aircraft

Various concepts for novel propulsion systems in regional applications have been explored in literature [3–5]. Orefice et al. [6] modeled an 8-propeller hybrid-electric aircraft with batteries and gas turbine engines, based on ATR42 mission requirements and geometric characteristics. They considered two propulsive lines, a primary one, consisting of the gas turbines and main propellers that can be assisted by an electic power on-take to the propeller shaft, and a second propulsive line consisting of an electric power train sourced by batteries and leading to the secondary propellers. The battery power was split among the primary and secondary propulsive line with different hybridization factors for different flight phases and nine operating modes were considered, in terms of combinations of thrust generation and energy harvesting by the propulsive lines. The battery discharge cycle was presented for the design mission and another typical mission. Finally, weight estimations were performed in the hybrid electric aircraft, and compared against the conventional, where a +51.7% increase in the OEW was predicted, and for a future 500Wh/kg energy density for the battery, a 51% fuel saving was predicted. Liu at al. [7] considered a hybrid regional aircraft retrofit with batteries and gas turbines, as well as a new aircraft design. The study included full mission analysis with time steps, and focused on aircraft-level design space exploration. to calculate the maximum range and fuel burn reduction for a range of hybridization factors and battery energy densities. Then, the case with the lowest battery energy density was isolated and a sensitivity analysis of the maximum range and fuel burn reduction to the cruise conditions was performed. A design exploration methodology for thin-haul and regional class charge-depleting parallel hybrid electric aircraft was explored by Cinar et. al [8]. A full mission analysis approach was considered, the motor-generator was modeled using a parametric, loss-based motor model from literature to obtain efficiency maps, battery pack-sizing was performed and a fixed efficiency was assumed for the converter and inverter. A 19-passenger and a 50-passenger aircraft were studied and the impact of technology variation and energy management on fuel burn was mapped. Concepts for low vs. high altitude climb e-boost and discharge strategy for batteries, electric taxi and battery usage schedules were considered.

2. *Fuel Cell Aircraft Concepts*

In terms of FC aircraft, under the MAHEPA project, Marksel et al. [9] performed mass estimations for a 19-seater FC aircraft using rapid and semi-empirical methods and estimated the mission fuel at conceptual level of analysis using the Breguet equation combined with electric component efficiencies for the SFC calculation. The authors considered both future optimistic and present pessimistic values for component power densities, efficiencies and other technological factors. They concluded that a 19-seater aircraft can be achieved with less MTOW than the conventional if the FC power density reaches 4 kW/kg. Several companies and institutes are also working towards developing the first FC-powered commercial aircraft. ZeroAvia is developing FC-powered electric aircraft of various classes and performed the first flight test of 6-seater demonstrator in 2020 [10]. H2FLY [11] has tested a 4-seater FC aircraft (HY4) in a 77-mile flight and reached an altitude of 7230ft for the first time, and aim to develop a 40-seater aircraft in the future. DLR and MTU are working on using the 19-seater Dornier 228 aircraft as a flying testbed retrofitted with hydrogen FC powertrains and aim for the first flight of the demonstrator to take place in 2026 [12].

C. CHARM

This paper presents a higher-fidelity, integrated framework within CHARM (Cranfield Hybrid-electric Aircraft Research Model) to model the mission performance of novel electrified propulsion systems tightly coupled with the overall aircraft system, enable emissions and energy consumption evaluation, heat management system detailed design and performance analysis at off-design conditions, electric power system and component design and performance analysis, and capture the interactions between the sub-systems and aircraft level. CHARM is the Cranfield Hybrid-electric Aircraft Research Model which is developed in the Centre for Propulsion and Thermal Power Engineering at Cranfield University to explore core technologies and synergies for electrified propulsion. It comprises elements of novel aircraft configurations and analysis [13–15], novel electrified architectures [16,17] (E-HEART), component and system dynamic behaviour, thermal management system analysis, component sizing, design and integration, emissions analysis, system diagnostic and health monitoring, multi-component life assessment [18,19] and asset management.

The purpose of CHARM is to develop an integrated approach to link the aircraft and operations with the subsystems and components of electrified propulsion. The design and performance analysis of electric power trains should be tightly coupled with the aircraft ecosystem, the flight mission, performance targets (ex. RoC) and operational constraints (ex. take-off distance, MTOW), to capture the special requirements, safety standards and the highly varying conditions that aerospace propulsion poses. Designing electric and hybrid electric systems for aircraft has additional challenges and safety implications than ground applications. Power and thrust requirements should be met within a wide range of conditions, from cold to hot conditions, from sea level to airports with higher elevation, from shorter airport runways to longer airport runways, and different cruise altitudes, pressures and Mach numbers, while minimizing energy consumption, emissions and mass, preventing component overheating, unexpected failures and FC oxygen deprivation and ensuring how much FC and electric component degradation can be tolerated with a given combination of aircraft and electric architecture. These targets cannot be achieved all to an equal extent at the same time, so the most feasible and beneficial trade-offs must be understood and selected. In that direction, higher-fidelity, integrated methods must be offered so that the design of the electric propulsion system and auxiliary systems (TMS, compressor etc) can be defined in synergy with the aircraft mission and performance targets (take-off length, cruise altitude, range, maintaining power targets under hotter conditions). Reversely, future operations (range, passenger capacity, service ceiling, degradation modes and maintenance requirements) unavoidably will be influenced and informed by the characteristics and constraints (mass, efficiency, energy, costs) of electric components.

The present paper focuses on the application of CHARM methods for the development of an integrated aircraft/engine mission analysis framework to design, model and understand the characteristics of a fully electric FC propulsion system.

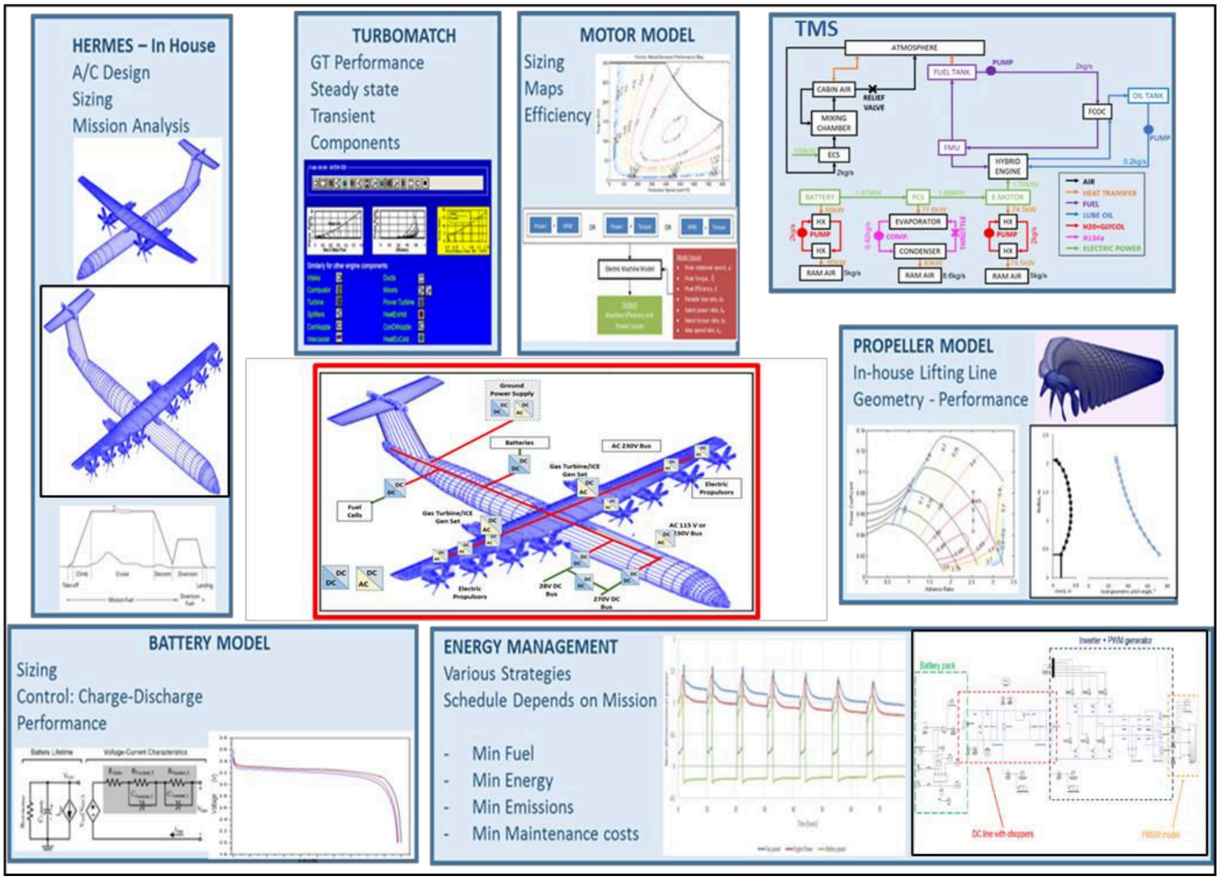

Fig. 1 Outline of the Cranfield Hybrid electric Aircraft Research Model

III. Methods

A. Aircraft/Engine Platform

The integration of the individual systems and the flight mission analysis are performed in Hermes, the in-house aircraft performance platform in the Centre for Propulsion and Thermal Power Engineering at Cranfield University. Drag calculations are performed based on the aircraft geometry and the aircraft acceleration and flight path calculations are based on the analysis of the acting forces on the aircraft. The weight of the aircraft is updated at each time step to account for the consumed fuel and the mission analysis is iterated until the mission target has been met (ex. calculation of fuel to achieve a fixed range with fixed payload). The development of Hermes has been described in more detail in [20]. For the analysis of conventional and hybrid gas turbine propulsion systems of any fuel type, the aircraft platform is coupled with Turbomatch, the in-house gas turbine performance code, which provides the engine operating conditions at each time step of the mission.

The baseline conventional aircraft for the present study is a regional aircraft model with geometry similar to ATR72 and twin turboprop engine models rated at 2MW each. A combination of publicly available data [21–23] and assumptions were used to create the models.

B. Propeller design and performance

The variable pitch propeller performance is simulated by using propeller maps produced with MIT's free tool Qmil/Qprop [24] for propeller design and propeller performance analysis which is based on an extension of the classical blade-element/vortex formulation [25]. The produced propeller geometry (chord length and pitch angle distribution along the blade span) and power coefficient map, along with the design steps, are demonstrated in Fig. 2. More background on propeller performance using Qprop can be found in [26]. The aircraft performance and mission analysis platform is generic and modular, so it can be combined with other propeller design approaches as well and incorporate maps from different sources.

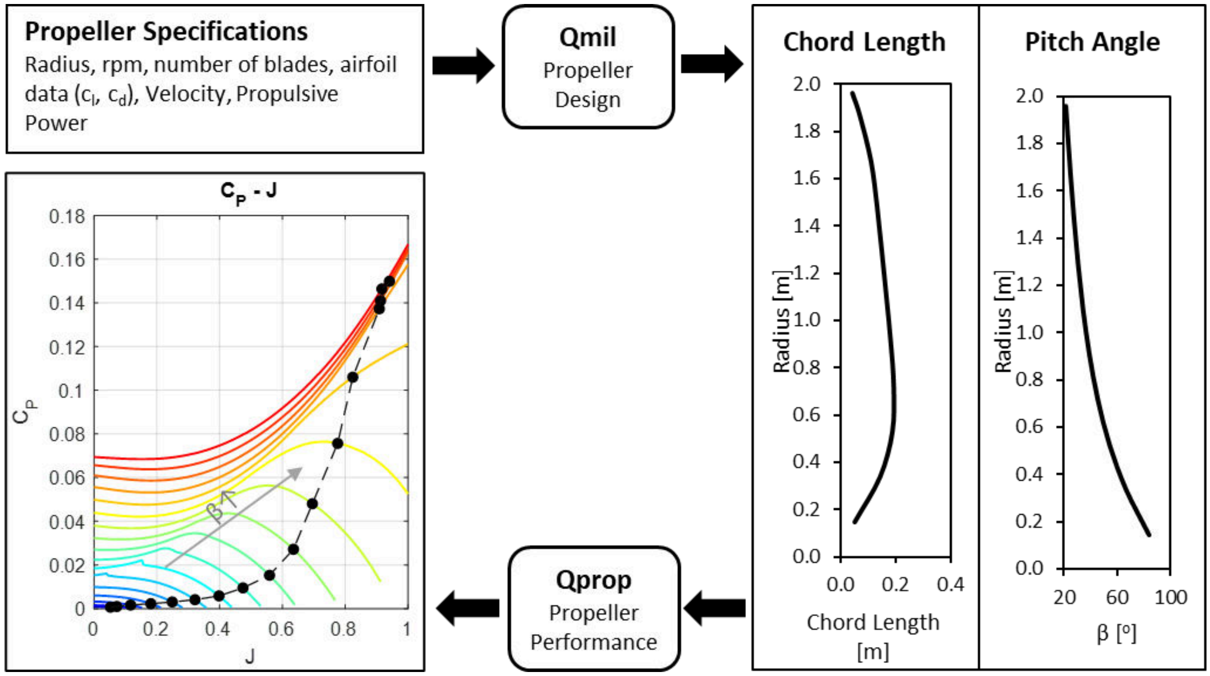

Fig. 2 Variable pitch propeller design & performance analysis (propeller geometry for baseline aircraft)

C. Gas Turbine Performance

The gas turbine performance is simulated with Turbomatch, the in-house gas turbine performance tool at Cranfield University. It is a component-based tool that resolves the operating point of the engine at design and off-design point, at steady and transient state, based on component maps, thermodynamic cycle calculations, conservation of energy, and conservation of mass and momentum. More information on the in-house gas turbine simulation tool is provided in [27].

The engine operating point can be handled with various parameters (TET, shaft rotational speed, required shaft power, fuel flow, etc). In the present simulation, the turboshaft model is handled with the TET to achieve the target power/thrust and, for the integration with the variable pitch propeller, the parameters in common are the shaft power and the relative rotational speed. The turboprop model is a combination of a turboshaft gas turbine model in Turbomatch, integrated with the variable pitch propeller maps that were produced with Qmil/Qprop [24]. The turboshaft engine model is rated at 2MW and was sized based on the available public data for PW127M turboprop [22,23], combined with assumptions for parameters that are not public.

D. Fuel Cell & Electric Power System

3. E-HEART – Electrical architecture design and performance

Based on the aircraft constraints, mission requirements, energy management strategies and failure cases, electric components are designed and matched to study different architectures either fully electric or combined with gas turbines (Fig. 3). The electrical architecture is modeled and analyzed with the in-house research tool E-HEART (Enabling-Hybrid Electric Aircraft Research and Technology), which is part of CHARM. Electrical components and their interactions at component level as well as their integration levels are studied within E-HEART. Different modeling approaches, from low-fidelity fundamental equations to high-fidelity models, such as finite element analysis for electric machines, and dynamic modeling of power electronics are included in E-HEART.

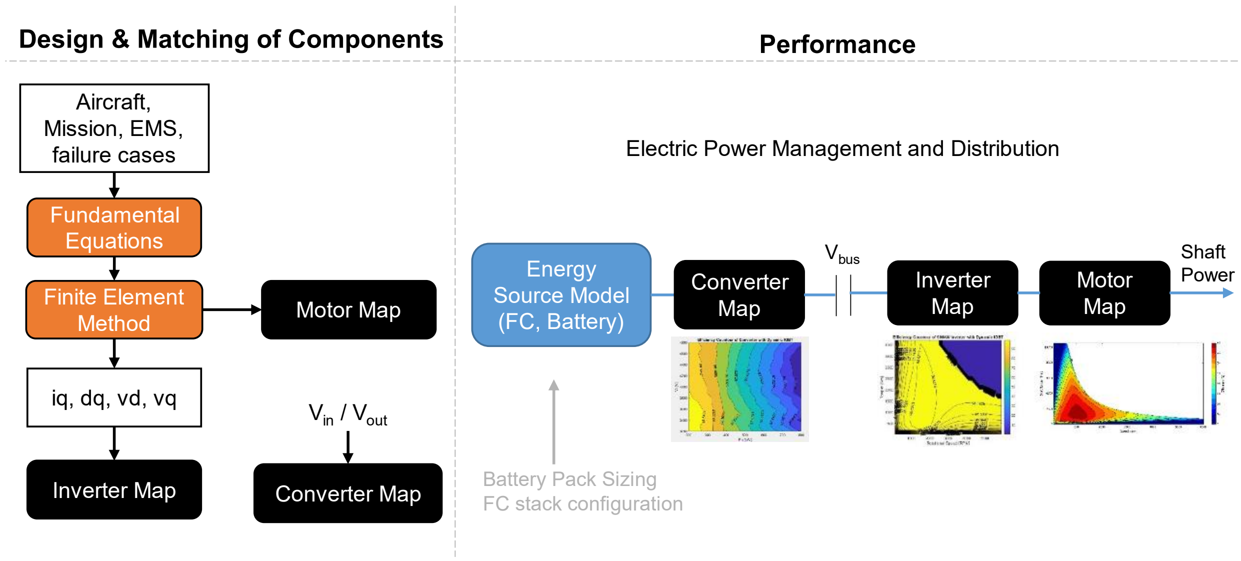

Fig. 3 Electric power system design and performance analysis

4. Selected Architecture

Selection of Number of Propellers/Motors

The baseline aircraft consists of a twin-turboprop propulsion system with 2MW rated power per GT, 3.93m propeller diameter and 1212rpm at 100% propeller speed. However, such high power (2MW) and low rpm (1212rpm) make the combination of torque requirement and low rpm very demanding, and the motor design becomes more challenging, resulting in heavier machines. In [28], the torque demand and rpm were calculated for a different number of propellers and a fixed maximum aircraft power requirement. The 8-propeller configuration is selected because it favors motor design at 500kW power requirement per propeller/motor and 2224rpm propeller speed without the need for using a gearbox.

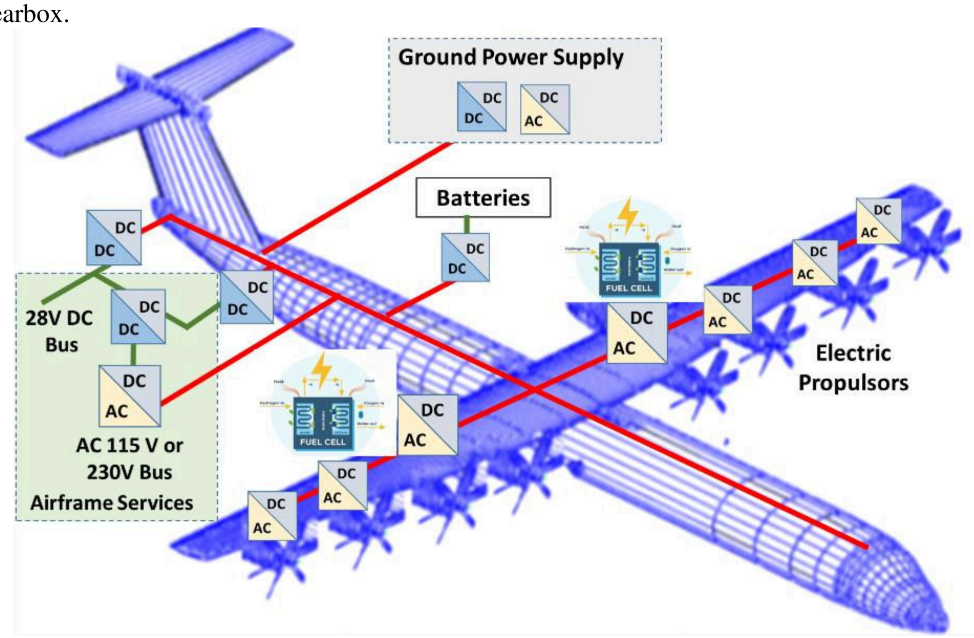

Fig. 4 Conceptual schematic of the 8-propeller FC aircraft

The 2224 rpm propeller speed is derived by scaling the baseline propeller while maintaining the same non-dimensional maps (C_P-J and C_T-J). When the propeller diameter is scaled by two (D=1.965m), the rpm can be doubled to maintain the same tip Mach number as a constraint. However, when the radius is divided by two, the area per propeller is divided by four because area is a function or squared radius. Furthermore, it should be noted that the propeller power/thrust is a function of CP/CT multiplied by area. Consequently, to operate with the same total power and total thrust at aircraft level with scaled propellers of half the radius compared to the baseline and same CP/CT maps, 8 propellers must be used to achieve the same total power.

Motor Design

For this study, fundamental equations and finite element analysis have been used for electric motor modeling. The Direct Quadrate (D-Q) modeling of Three-Phase Permanent Magnet machine is used to control and design an H-bridge inverter. The electric motor efficiency map is obtained from a 2D FEA-based solution in ANSYS Motor-CAD. The power electronic is modeled based on existing component models and the efficiency contours are obtained [29]. More details on the motor design by the authors are presented in [28]

Voltage selection

The selection of system voltage for the electric powertrain has been studied with considering the trade-offs between, weight reduction (ex. cable's weight, where lower total weight is expected for higher voltages), and at higher voltage and increasing altitude the occurrence of arcing increases as a result of the decrease in the breakthrough voltage with decreasing surrounding air pressure, or the reduction of conduction and Ohmic losses in power electronics and electric machines but with an increase of switching losses due to high voltage demand, and lack of high power density protection systems for high voltage distribution.

A fixed 2000V DC-bus voltage was selected as a system voltage below the 3000V voltage threshold identified in [30] for operating at a safe voltage at high altitude for regional aircraft. In a study conducted by Vratny et al. [31], for a constant system voltage architecture in a 6MW powertrain optimum system, the voltage was identified at higher voltages, between 3000V and 4000V. In the present study's electric motor design exploration, voltages higher than 3000V led to higher increase in winding insulation and reduction in current flow in the winding and the challenges in cooling the winding, hence the electric machine design was not explored above 3000V for a 2MW powertrain.

Converter and FC configuration selection

The selection of the fuel cell configurations and the DC-DC converter is based on the study conducted in [17] out of which a configuration with higher reliability has been selected. Designing a protection system for four fuel cell stacks in series with lower current in comparison with four stacks in series and parallel is recommended. The four DC-DC converters that are used for voltage control can potentially be removed from the selected architecture (Fig. 5) with a slight benefit (max 2% increase) on total system efficiency and also reducing total weight from four converters as discussed in [17]. In this paper, the more reliable architecture with four converters was selected, but in future work, the effect of the converter removal on the aircraft and mission performance can be explored.

A Proton Exchange Membrane Fuel Cell (PEMFC) stack with a maximum power of 150kW is selected based on an existing commercial product (FCvelocity®-HD6 PEMFC) and modeled based on the experimental results shown in [32]. As part of the FC auxiliary system, a compressor is considered that provides the required airflow at the nominal operating pressure of the FC. Sixteen stacks are added in different configurations to provide up to 2.4MW FC output power, which is sufficient to convert to 2.05MW output shaft power from the motors. The rated power of the conventional propulsion system (GT) is 2.05MW and corresponds to half of the power required for this aircraft. Another sixteen stacks are connected to a second bus to provide the total of 4.8MW FC output power (4.1MW output shaft power) required by the whole aircraft as shown in Fig. 5. The fuel cell stacks are connected in a configuration (4 parallel and 4 in series) that reduces the failure rate due to degradation of one of the stacks or the incompatibility between the stacks, which was studied in [33]. More details on the FC modeling and equations are provided in [33].

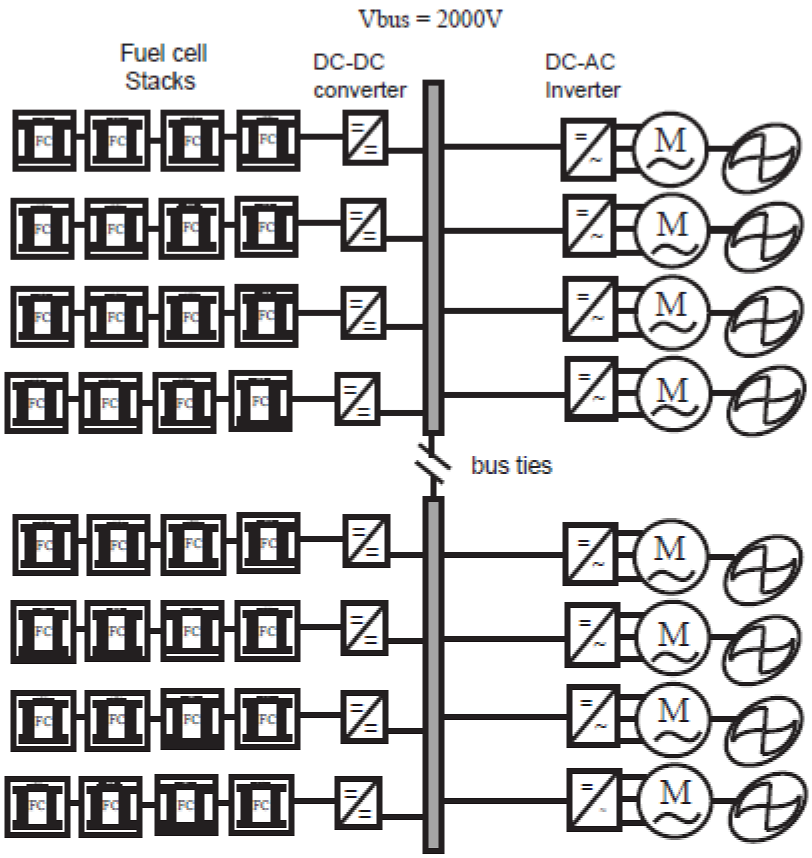

Fig. 5 The proposed propulsion system with FC stacks at high voltage. A DC/DC converter is used to maintain the bus voltage at 2000V.

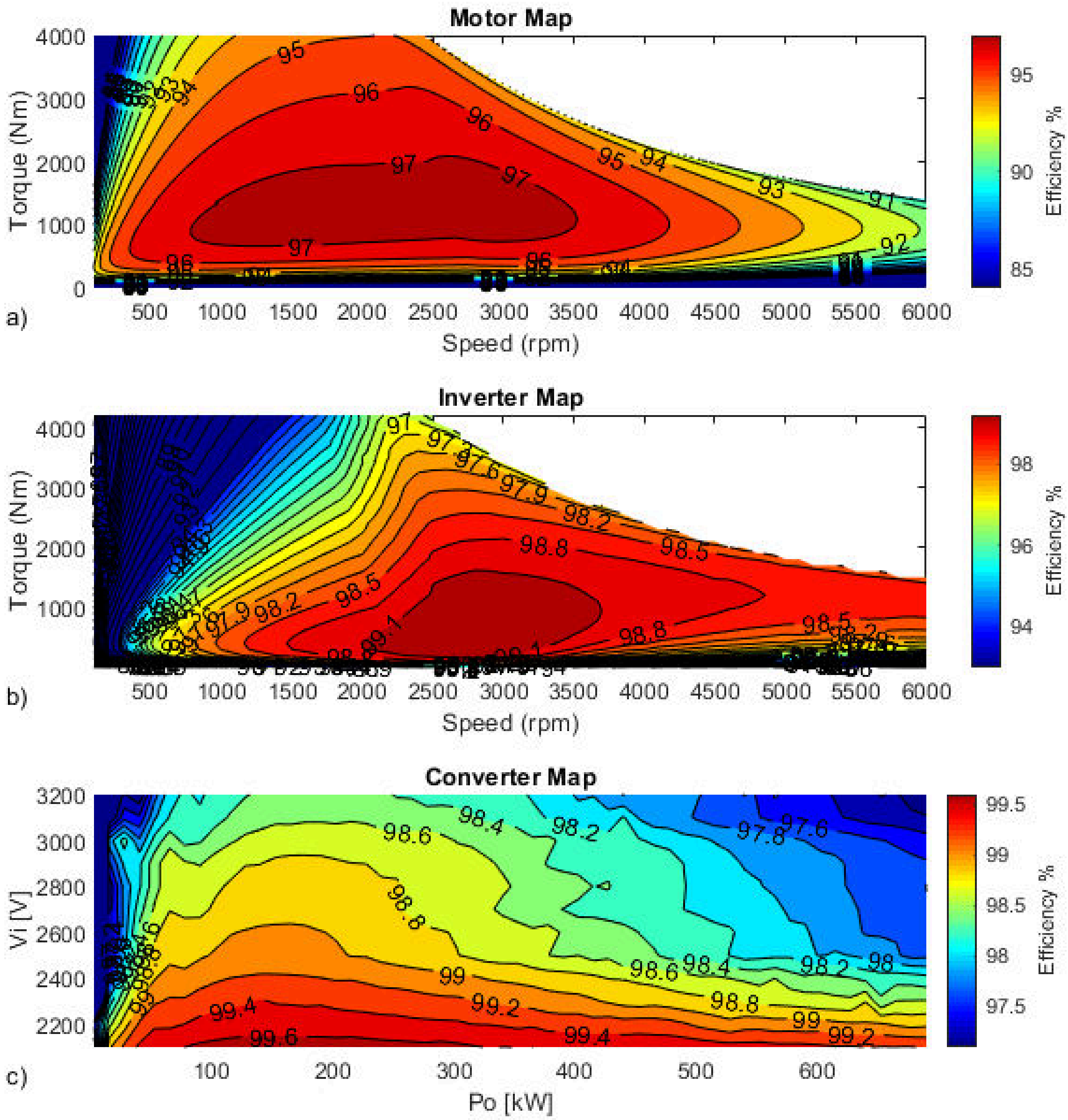

Fig. 6 Maps of the selected electric component designs for the FC fully electric propulsion system a) Motor Map b) Inverter Map c) Converter Map

5. Thermal Management System

FC as a power source for aircraft propulsion offers significant benefits in terms of emissions reduction but they have major issues with heat generation since their heat losses are in the order of magnitude of 50% of their input power. Specifically, for a ~4MW FC propulsion system as the one modeled and assessed in the present paper, the heat loss rate can be as high as 4MW at take-off. Consequently, a need arises for heat management solutions with the lowest possible Thermal Management System (TMS) weight.

Depending on the operating temperature of the FC, either a liquid cooling loop or a vapor cycle loop can be used as TMS. Typically, a minimum temperature difference of 7-10 °C is required on the hot and cold side of heat exchangers. Considering a hot-day take-off condition, the ram air will be at 45 °C. In this case, the minimum operating temperature of FC allowed with liquid cooling loop will be 65 °C. Higher operating temperature results in lower heat exchanger weight, since the required heat transfer area is reduced for the same heat load and overall heat transfer coefficient. Assuming the operating temperature of the 4MW FC is at 65 °C, the TMS weight with aluminum heat exchangers will be around 1600 kg with a liquid cooling TMS of 2-3kW/kg heat dissipation effectiveness [34].

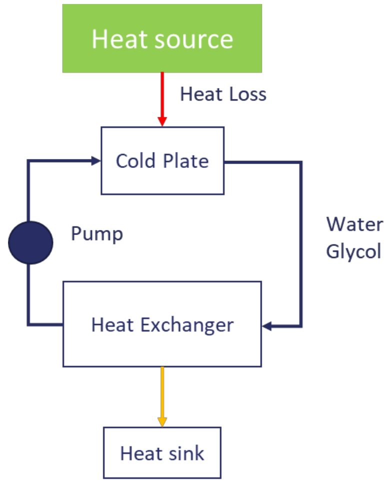

Fig. 7 Liquid cooling system for thermal management system

Since the FC is marginally a low-grade temperature heat source for liquid cooling loop, a vapor cycle loop can be added to make sure the heat is dissipated at extreme ambient conditions with low-speed ram air at hot-day take-off. This architecture is shown in [35]. Adding VCS increases the temperature difference on hot and cold side of heat exchangers leading to a significant reduction in TMS weight by 800 kg [34]. However, the refrigerant compressor will need 1MW of power when the heat load is 4MW. The ongoing research on TMS is expected to address the weight issue and make FC-only propulsion more feasible. It should be noted that a more detailed analysis and modeling of the candidate thermal management systems is out of scope in this paper, but one of the outcomes of the research presented in the paper is to inform the design of the heat management system and its off-design performance analysis.

E. Integrated Mission Performance Analysis Platform

The flight mission and aircraft performance platform is coupled with the turboshaft - propeller propulsion system. The flight mission provides at each point the altitude and Mach. A setting for the relative rotational speed of the propeller and turboshaft power turbine is also an input. The absolute rpm of the power turbine and the propeller are not the same, a gearbox with a fixed reduction ratio 18 is considered, but the relative rotational speed is considered always the same. Consequently, the relative rotational speed is input to both the propeller model and gas turbine model. The gas turbine operating point is also handled to provide the necessary shaft power to the propeller. The gas turbine operating point and power output, for known Mach and altitude, can be handled with either spool speed, fuel flow or TET. In the present paper, the simulation handle is the TET. The Mach number and altitude provide aircraft velocity in terms of true airspeed and along with the relative speed input (100% rpm is known), the advance ratio of the propeller at the given operating point is calculated. The gas turbine shaft power output is also input to the propeller. Air density is known from flight mission altitude, so the power coefficient is calculated. With the power coefficient and advance ratio being known, the pitch angle can be identified from the propeller C_P-J map. Then, the thrust produced by the propeller can be calculated from the C_T-J map based on the advance ratio and pitch angle. The propeller thrust is added to the gas turbine exhaust thrust and is returned to the flight mission analysis along with the GT fuel flow. Consequently, the aircraft performance code can update the aircraft weight at the next time step and can calculate the acceleration/deceleration of the aircraft from the propeller and gas turbine thrust sum. At cruise, where there is steady non-accelerated flight, the gas turbine power is iterated until the sum of the propeller and gas turbine exhaust thrust can balance out the drag of the aircraft.

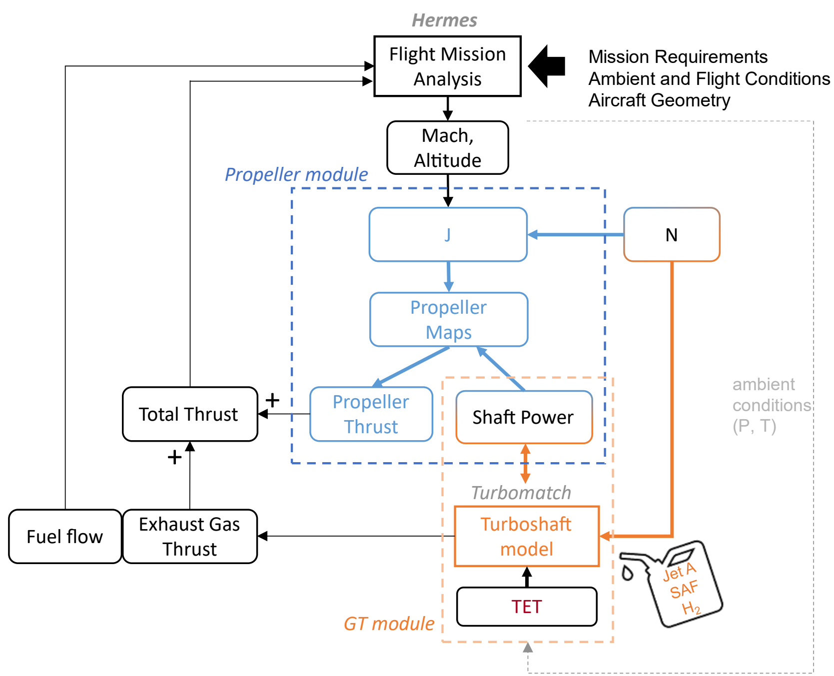

Fig. 8 Integration flowchart for GT-Variable Pitch Propeller-Aircraft system within the flight mission analysis platform

Similarly, when the propulsion system is FC-powered the integration flowchart converts to Fig. 9. The gas turbine propulsion system is replaced by a fuel cell – electric powertrain propulsion system as the shaft power source. The methodology that connects the elements of propulsion is similar to the previous Fig. 8 but the main difference is that this time the only source of thrust is the propeller thrust, gas turbine exhaust thrust is not present anymore, and the fuel flow that is returned to the flight mission analysis for the weight calculations is the fuel cell hydrogen consumption.

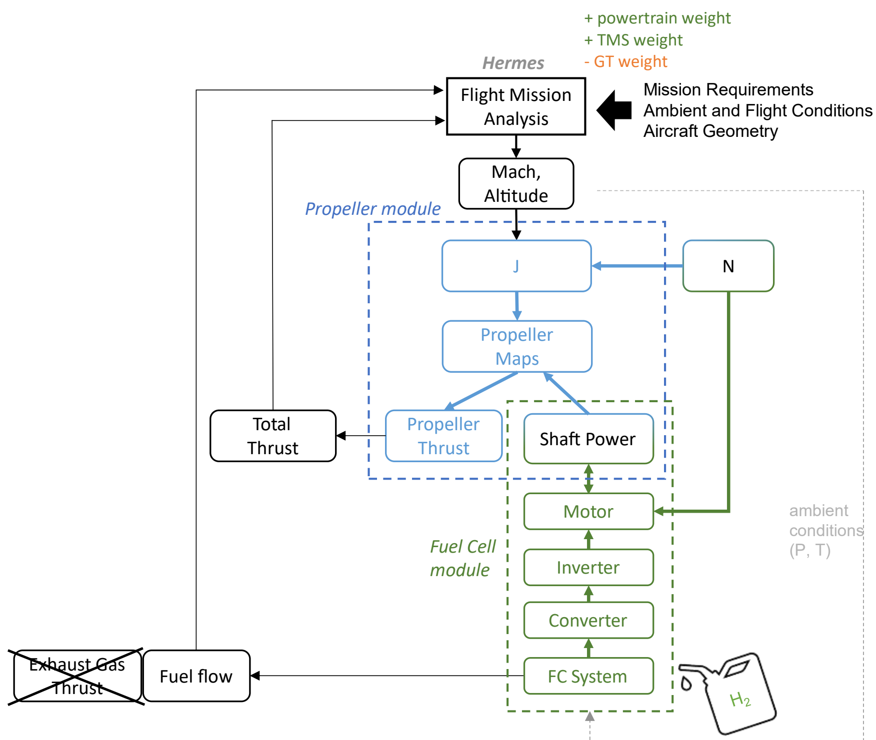

Fig. 9 Integration flowchart for FC system-Variable Pitch Propeller-Aircraft within the flight mission analysis platform

F. Preliminary Weight Estimations

The FC propulsion system and the hydrogen gas turbine are retrofitted to an aircraft model similar to a 70-pax regional aircraft of today. The retrofit approach is considered for two reasons:

1. It narrows down the already wide design space of electrified propulsion by removing the aircraft geometry as a variable. In this way, the present analysis can focus on the novel propulsion system attributes and its interaction with the airframe as a constraint.
2. Retrofitting existing aircraft with novel propulsion systems may offer environmental benefits in a shorter timeframe because the development, testing, certification and large-scale production of clean-sheet aircraft designs require additional time and expensive investments. Although a clean sheet design can be developed to offer optimized solutions and maximized benefits, it will take many years and high costs to produce the new aircraft and replace all operator fleets. Retrofitting can potentially serve as an intermediate step of a phased transition since there are large fleets of existing aircraft that are fully operational, have long remaining life and would take many years to be replaced with new aircraft. Black et al [36] discussed the benefits of retrofitting existing fleets with more efficient engines as a nearer-term solution and the considerations to be taken into account when choosing between clean sheet designs and engine retrofitting. In the context of retrofitting with more disruptive electrified technologies there are even more challenges to overcome, but it remains an attractive intermediate step.

In this analysis, the updated Operating Empty Weight (OEW) of the FC retrofit aircraft considers the removal of the GTs as the system is purely electric and the additional weight of the FC system, the electrical system, the hydrogen tank and the thermal management system. In this paper, the effect of replacing two big propellers with eight smaller propellers will be ignored, so the same propeller mass is assumed. Overall, the change in propeller mass is expected to be of secondary importance compared to the effect of the FC and electric system weight on the OEW.

$$OEW_{FC\ Retrofit} = OEW_{conventional} - W_{GTx2} + W_{FC} + W_{electrical\ system} + W_{H_2\ tank} + W_{TMS} \quad (1)$$

$$OEW_{H_2\ GT\ Retrofit} = OEW_{conventional} + W_{H_2\ tank} \quad (2)$$

Since this is a retrofit approach, the conventional aircraft OEW and gas turbine weight are based on typical values found in the public domain for 70-pax regional aircraft and 2MW turboprops of similar class. The enabling technologies for a future fuel cell propulsion system, such as lighter TMS technology and electric components with high power densities, have not reached the required technology level yet. For this reason, future (2035) technological factors should be assumed for the aircraft and system weight estimations (Table 1) based on value ranges reported in literature and roadmaps [35,37–41].

Table 1 Technology factors

	Future - 2035	Current
Low-Temperature PEMFC power density	1.5 – 3 kW/kg	0.3 - 0.5 kW/kg
Motor power density	10-16 kW/kg	2 kW/kg
Power electronics power density	10-16 kW/kg	2.2 kW/kg
TMS cooling effect per system mass	2-3 kW/kg	1 kW/kg
Hydrogen tank gravimetric efficiency	50% - 70%	-

A retrofit approach to an existing aircraft platform requires adherence to two types of constraints:

- Mass constraint: This means maintaining the same MTOW as the baseline aircraft so that the maximum wing loading does not change. This is achieved by reducing the payload when additional system mass is required (ex. electrical components, fuel cell, TMS and hydrogen tank in the case of the fuel cell retrofit)
- Volume constraint: This constraint regards the available cabin volume, where the cryogenic hydrogen tank is expected to be placed. Hydrogen has a very low density and even in the cryogenic form, it occupies approximately 10-11 times the volume of equal kerosene mass. In the present study, the fuel cell and electrical system volume is not a part of the volume constraint, as these parts are expected to be placed under the wing, replacing the conventional gas turbine.

The passenger reduction due to the mass constraint is compared with the passenger reduction due to the volumetric constraint (hydrogen tank volume) and the payload/passenger reduction is the maximum out of the two. It is considered that the average passenger weight is 95kg and the cabin volume that one passenger occupies is $0.82m^3$. The cabin volume that corresponds to one passenger is estimated by the cabin cutaway surface of a typical 70-pax regional aircraft [13] multiplied by the seat pitch (0.76m). In the case of the hydrogen gas turbine, the dominant constraint is the volumetric, as the only additional weight is that of the hydrogen tank. Consequently, the payload reduction is driven by the volume requirement for hydrogen storage.

In this paper, the mission analysis of the FC aircraft is performed with the MTOW. Due to the uncertainty in the progress of the enabling technologies, the effect of technology factor advancement and the weight estimations presented in this section are incorporated in a parametric analysis for the calculation of the energy per passenger.

IV. Findings

G. Mission Performance

1. Aircraft Performance

The mission performance characteristics of the FC retrofitted aircraft are analyzed over flight time The basis for comparing the three technologies (FC, hydrogen GT, conventional GT) is to achieve the same mission (300nmi, 19000ft cruise altitude and MTOW) and performance of a typical regional aircraft. Consequently, the flight profiles (Mach and altitude) nearly coincide in all three cases (Fig. 10). Aircraft performance requirements are usually set at take-off, climb and cruise so the aim in this study is to achieve those requirements. The descent profile is not constrained so the descent time varies based on the different aircraft weights at the end of cruise (Fig. 11a).

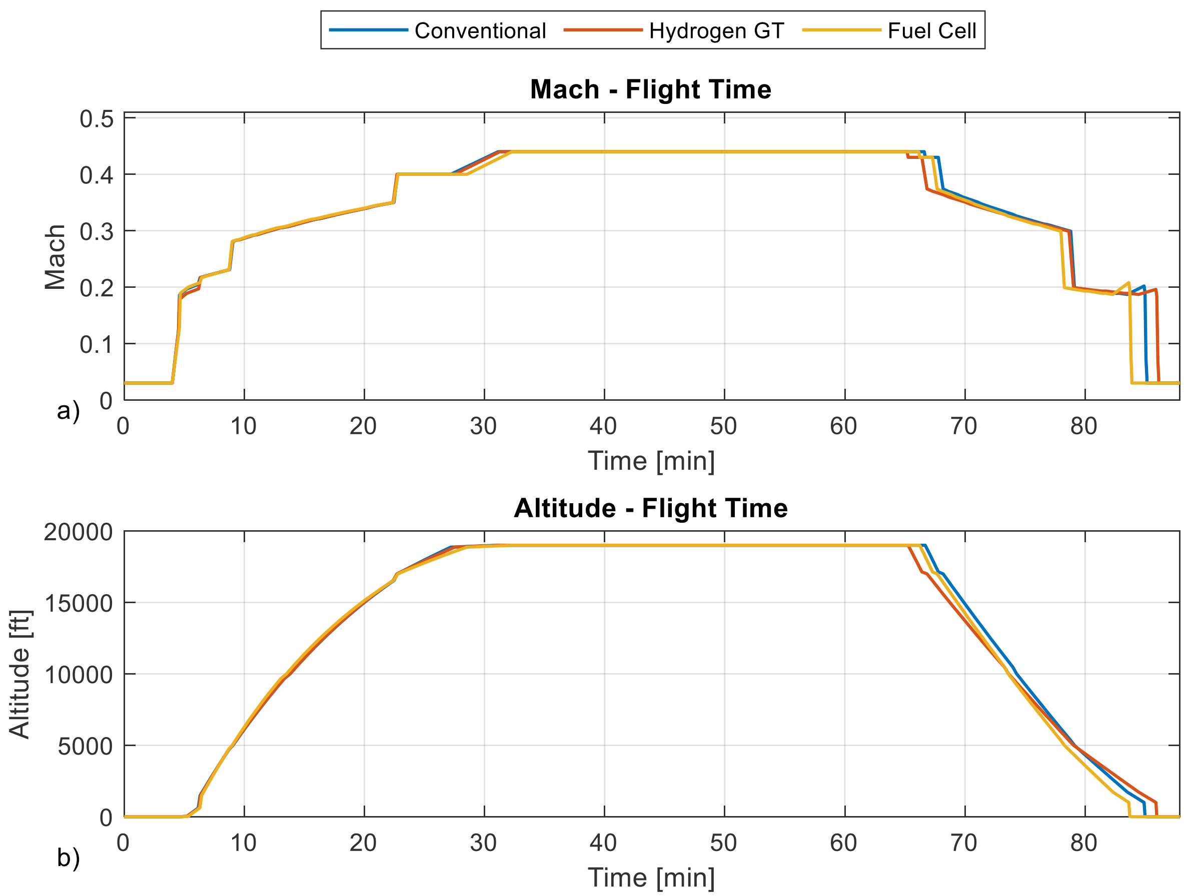

Fig. 10 Flight mission profile (Mach and Altitude)

When performing the same mission, the fuel cell aircraft weight is higher than the conventional and hydrogen gas turbine, due to the additional FC system weight. The FC fuel weight will be less though than the kerosene aircraft, but for this application, this fuel weight reduction is not enough to overcompensate for the additional FC system weight. Due to the higher fuel consumption of the conventional gas turbine, it is observed that the aircraft weight of the conventional weight has a more aggressive gradient over the flight, compared to the hydrogen aircraft that has a very slow weight reduction. The target was to achieve the same flight path so the power setting was adjusted so that the same RoC is achieved in all cases. These observations should be considered in the sizing of fuel cell propulsion systems as well as new aircraft designs. For instance, the Top of Climb (ToC) weight of the FC aircraft will be very close to take-off weight, in contrast with conventional kerosene aircraft that have burned a few hundred kilograms of fuel during take-off and climb, and thus have a lighter ToC.

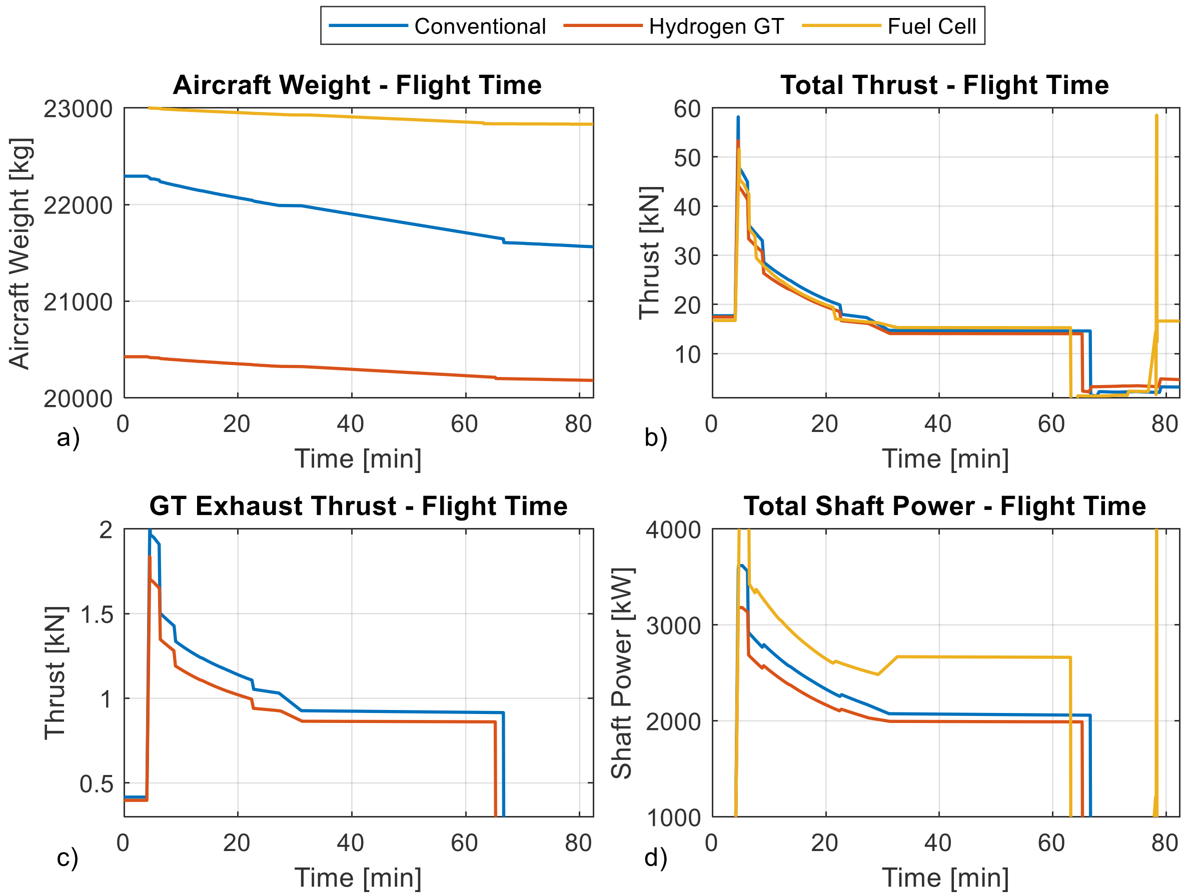

Fig. 11 Aircraft performance parameters over flight time

2. Variable Pitch Propeller Performance

As demonstrated in Fig. 11, the FC aircraft has a higher weight than the conventional, when performing the same mission, consequently, its thrust requirement increases. Adding to that, the gas turbine exhaust thrust is not present anymore, so the fuel cell power has to further increase so that the propellers can provide 100% of the required thrust to maintain the same aircraft performance and flight path. Finally, the fuel mass consumption of the FC aircraft is about 4 times lower than the consumption of the conventional, so the FC aircraft weight reduces more slowly over the mission compared to the conventional.

To produce more propeller thrust to compensate for the effects discussed above, the propeller pitch, power coefficient and thrust coefficient are higher for the heavier fuel cell aircraft (Fig. 12). The advance ratio is similar for all aircraft because the aircraft velocity and the circumferential velocity of the propeller tip are maintained the same (in the case of the 8-propeller configuration the propeller is scaled from the baseline in a way that the tip Mach number is the same).

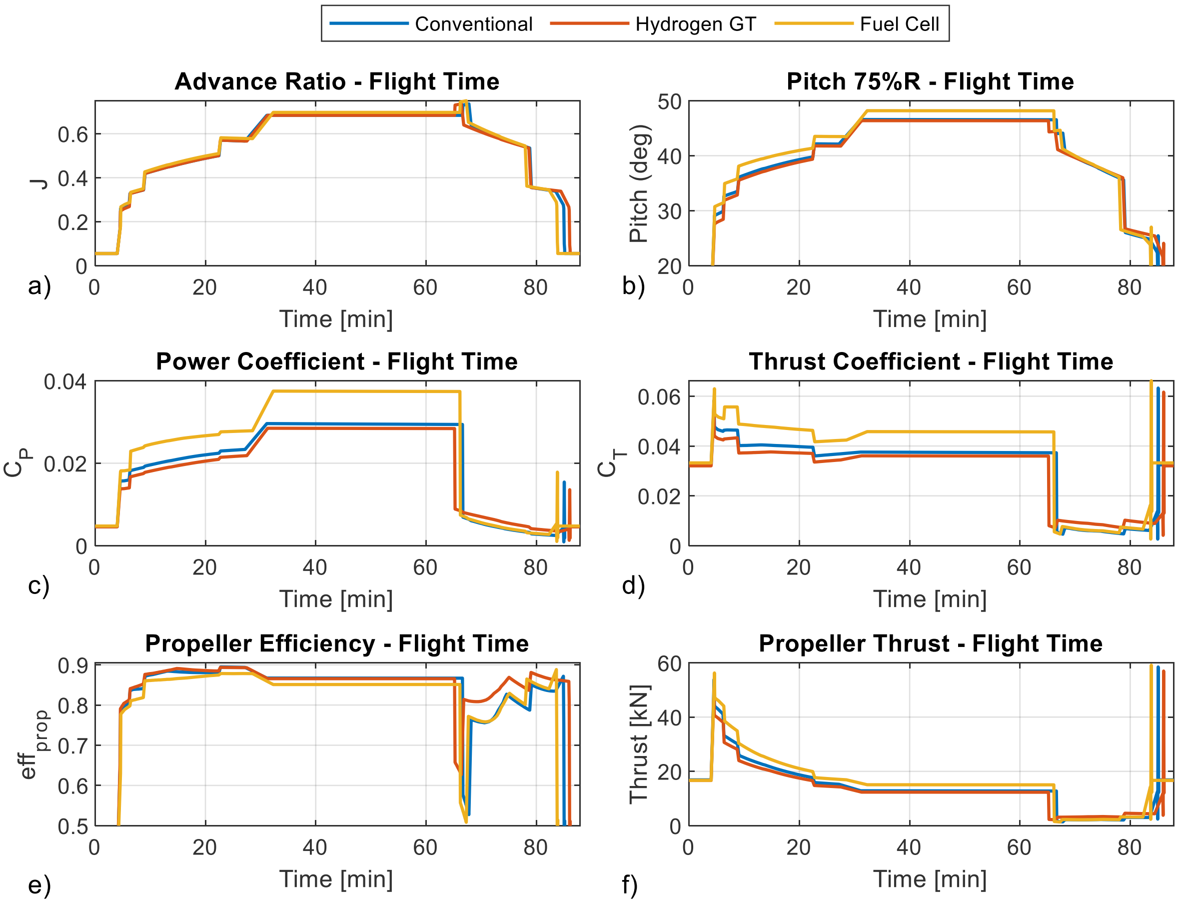

Fig. 12 Variable pitch propeller performance over flight time

3. Gas Turbine Performance

Apart from the lighter aircraft weight, the hydrogen gas turbine operates at a lower TET than the kerosene conventional gas turbine, because hydrogen combustion products have higher specific enthalpy than kerosene combustion products. For the same reason, the hydrogen gas turbine exhibits up to 0.6% higher turboshaft thermal efficiency than the kerosene gas turbine, despite the higher TET for the conventional GT. The higher temperatures lead to slightly higher kerosene GT exhaust thrust at take-off, but the difference becomes even smaller during cruise. However, the power requirement of the fuel cell aircraft is considerably higher (+742kW at take-off) than the kerosene gas turbine, when performing the same mission due to the additional aircraft weight and the loss of GT exhaust thrust, which means that the propeller must operate at higher power settings to provide alone the increase thrust requirement of the additional weight and supplement the GT exhaust thrust.

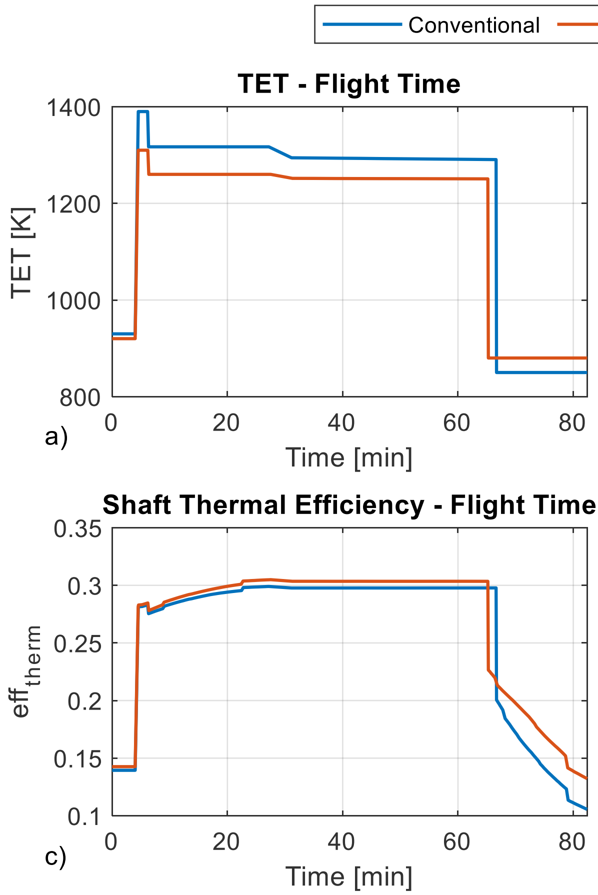

Fig. 13 Conventional and hydrogen gas turbine performance

H. Overall Propulsion Performance Assessment

Fig. 14f compares the total propulsion of the three technologies, which is defined as the propulsive power over fuel input power. First, it is observed that the morphology of all the propulsion efficiency curves follows the morphology of the propeller effiiciency curve during the mission (Fig. 14a). The FC aircraft has the highest propulsion efficiency because it has the lowest fuel and energy consumption out of the three aircraft (Fig. 14c and d) along with higher thrust at ToC and cruise. The hydrogen gas turbine has slightly higher propulsion efficiency than the conventional gas turbine. The hydrogen gas turbine is slightly more efficient than the conventional (Fig. 14c) and the fuel flow is significantly lower than the conventional (Fig. 14c and d), however due to the high energy content of hydrogen, the difference in fuel input energy becomes small and ultimately the propulsion efficiency of the hydrogen gas turbine is only slightly higher than the conventional (Fig. 14f). Finally, another interesting observation is that the efficiency curves in Fig. 14b are nearly mirrored. The gas turbine is more efficient at the the phases with high power (take-off, climb, cruise) and the efficiency improved at higher altitudes from take-off to cruise, while the FC system is more efficient at the phases with lower power settings (taxi and descent), while take-off becomes the phase with the lowest FC efficiency.

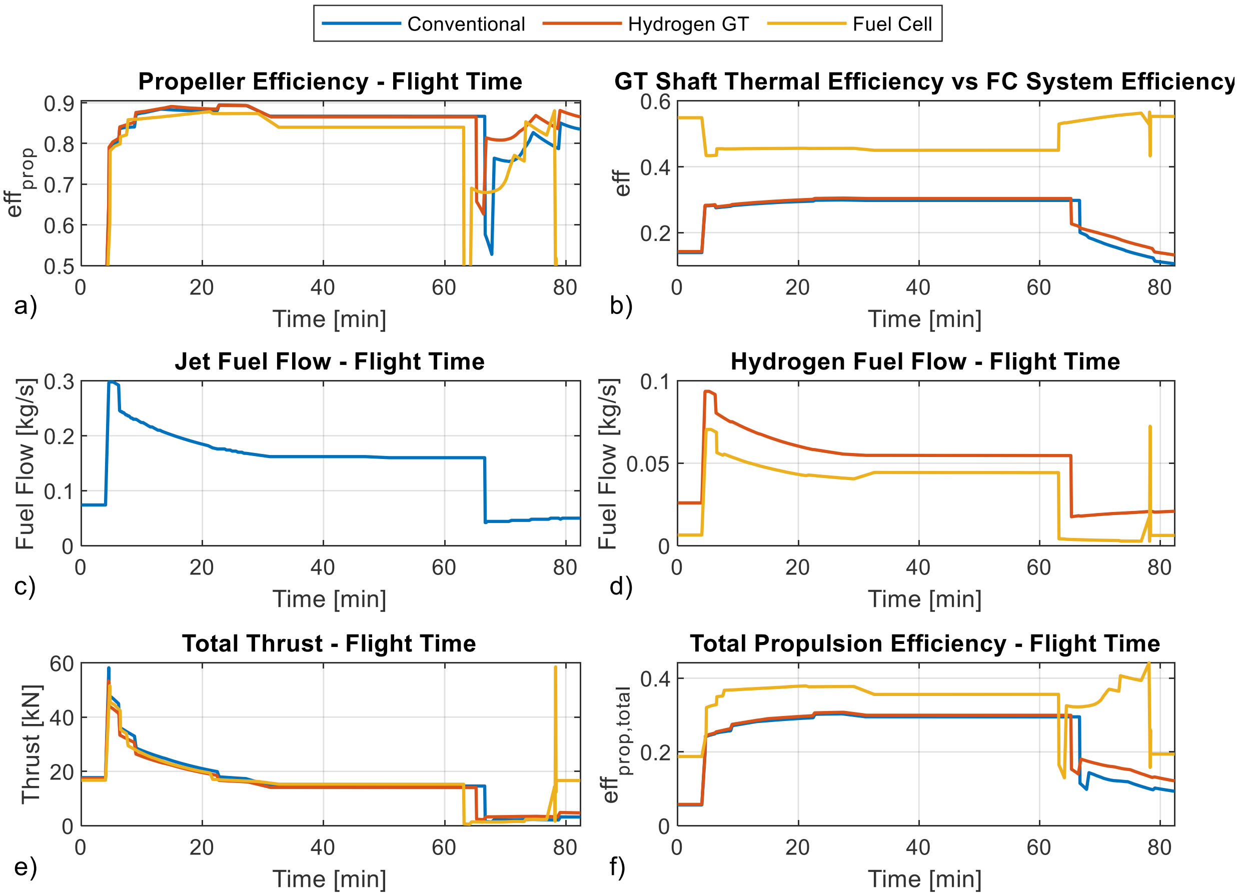

Fig. 14 Overall Propulsion Performance Assessment

I. Emissions

The NOx emissions of the conventional aircraft are calculated using the widely used P_3-T_3 method [42], which is a semi-empirical approach based on reference emission data at sea level corrected for the ratio of P3, T3 and FAR between sea level and flight level. Representative emission indices for a turboprop engine [43] of similar class to the model considered in this study are used in the calculations. The CO_2 and H_2O emissions from jet fuel combustion are considered proportional to the fuel burn with ratios of $3.16 kg_{CO2}/kg_{fuel}$ [44] and $1.23 kg_{H2O}/kg_{fuel}$ [45] respectively. The H_2O mass flow rate produced by the hydrogen combustion and FC electrochemical reaction is calculated based on the H_2O moles than can be formed when the moles that correspond to the H_2 fuel flow react with an excess amount of oxygen that allows full conversion. This calculation provides a production factor of $9 kgH_2O/kgH_2$.

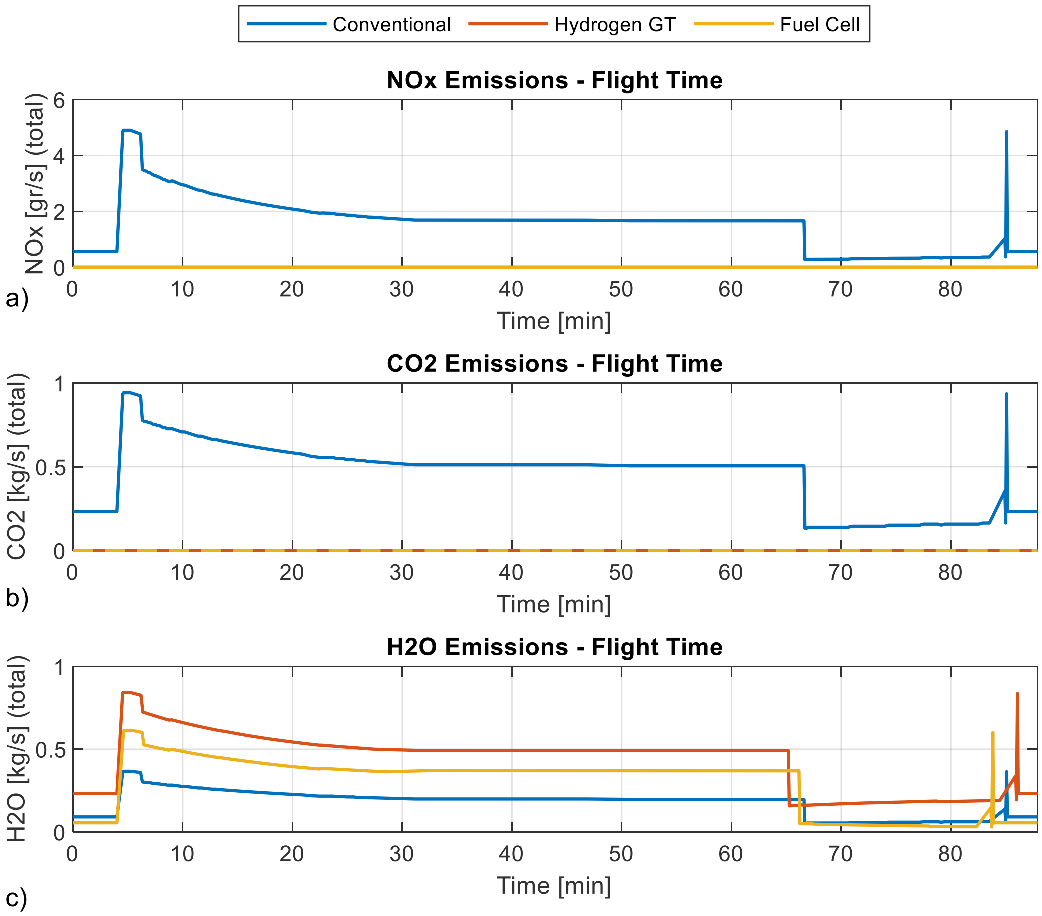

Fig. 15 Emissions produced by the conventional regional aircraft, the hydrogen GT aircraft and the FC fully-electric aircraft

J. Energy consumption per flight phase

The relative fuel/energy burn per flight phase for each aircraft technology is presented in Fig. 16. The fuel cell system results in a lower relative fuel burn at taxi and descent because the fuel cell is more efficient at the phases with lower power settings. Reversely, both gas turbines, irrespective of fuel, are more efficient at high power settings so the relative fuel burn at take-off and climb are lower than the fuel cell.

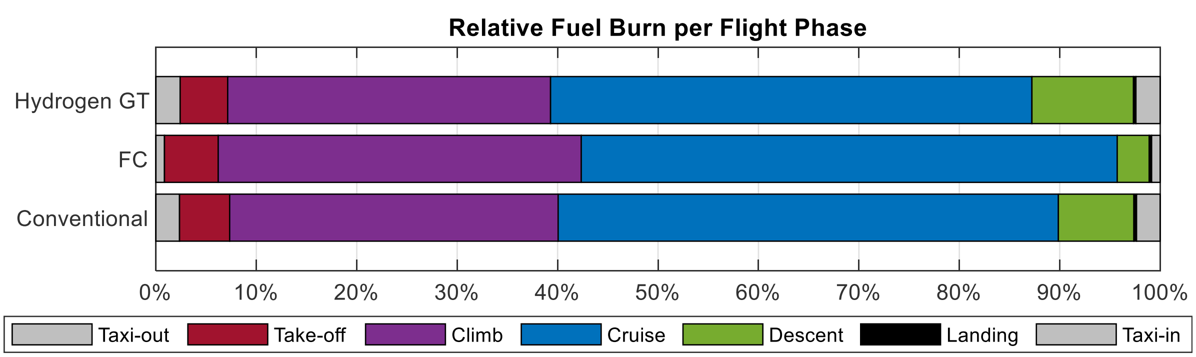

Fig. 16 Relative fuel/energy consumption per flight phase

Moving to mission energy, for the investigated, representative mission, the fuel cell aircraft offers a 26.47% reduction in flight energy consumption compared to the conventional 70-pax and the hydrogen gas turbine offers a 6.11% flight energy reduction, as it is less efficient than the fuel cell. In-flight NOx and CO_2 emissions are eliminated which makes FC propulsion an attractive candidate concept. The flight NOx for the hydrogen gas turbine retrofit is not included in Fig. 17b because of the limited information but there is ongoing research to address the design and NOx emissions of hydrogen combustion technologies. For this mission, the water emissions of the FC aircraft are higher than the conventional aircraft but lower than the hydrogen gas turbine, because the FC system has higher efficiency than the hydrogen gas turbine.

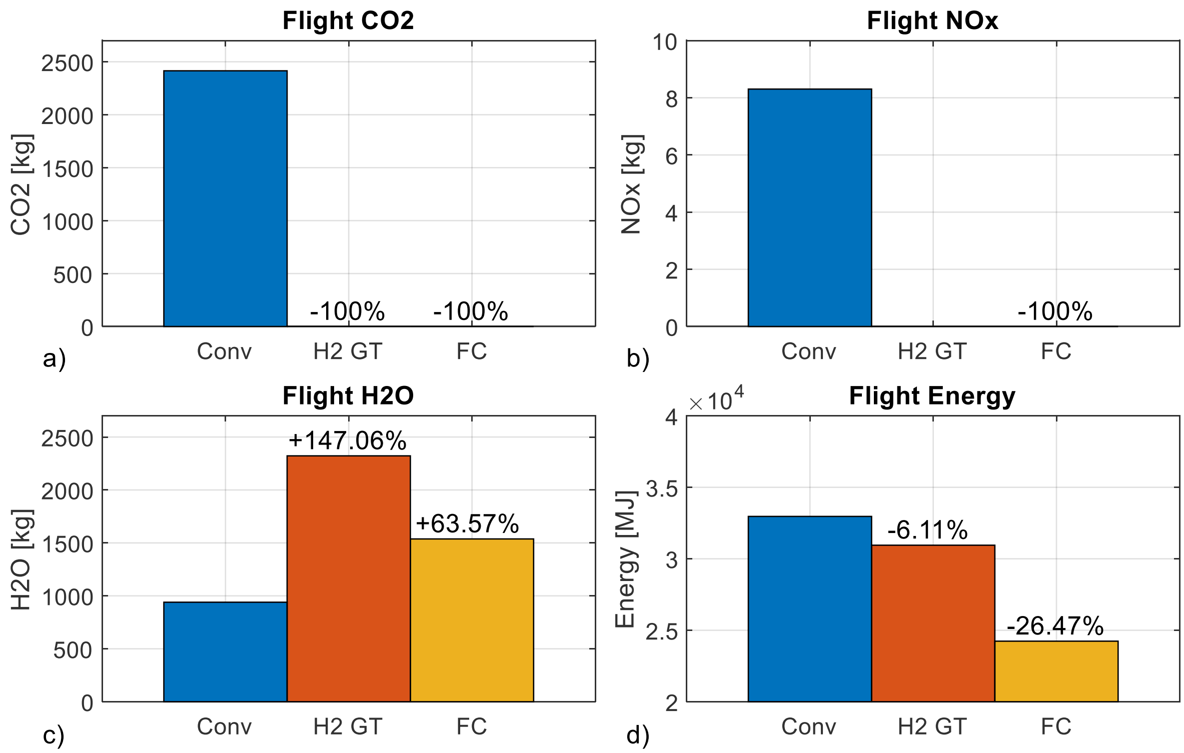

Fig. 17 Fuel and Fuel Energy Savings for each technology

K. Uncertainty analysis on the advancement of technology factors

Despite the energy reduction at aircraft level (Fig. 17d), the equivalent energy per passenger may be a more meaningful metric to evaluate the energy performance of aircraft with different propulsion systems. The amount of feasible payload and number of passengers (pax) depend on the advancement of the enabling technologies. The 300-nmi mission was performed with MTOW, which is used as the constraint for the sum of the operating empty weight (OEW), TMS, electric system, FC system mass, propellers, tank mass, fuel on board, including reserves, and payload which can be translated into passengers in the context of a commercial aircraft.

The mass of the designed electric components and FC configuration, which are based on models and technology factors available today, will not be extensively discussed in this paper. The scope for this paper is focused on the integrated mission performance analysis using the component maps. The additional system mass and resulting aircraft weight are treated in an uncertainty analysis. In this uncertainty analysis, the propulsion system mass is traded-off with passengers and payload, while the MTOW constraint is maintained. The TMS cooling effect (heat dissipated per mass of TMS), the FC, power electronics and motor power density (power per system mass) are varied within a range that covers today's state-of-the-art and future predicted values.

The total flight energy of the FC aircraft for the 300nmi in Fig. 17d is considered. That mission was performed with MTOW. A new OEW is calculated for each combination of TMS, FC, motor and power electronics power density from Fig. 18 using Eq. (1). The MTOW is maintained as a constraint, so for each combination of technology factors, a new payload allowance is calculated as the difference of the new OEW and on-board fuel from the MTOW. The new payload allowance is divided by a typical mass per passenger (95kg) to obtain the passenger capability in Fig. 18a. The propulsion system delivers the required power and thrust for the MTOW and the given flight conditions, and its behavior is not affected by how the MTOW is distributed between payload and OEW, so the total flight energy is always the same and is not affected by the power densities. The total flight energy of the FC aircraft (Fig. 17d) is divided by the number of passengers (Fig. 18b) to obtain the energy per passenger in Fig. 18b.

The blank area of the chart indicates technology factor combinations that their resulting aircraft weight did not allow more than 10 passengers to be carried in the 70-passenger aircraft retrofit, as this increases the energy per passenger excessively and is considered an unacceptable solution. Around the lowest power densities, there were even points at which the MTOW should be exceeded to carry the propulsion system. Despite the elimination of direct carbon and NOx emissions, a fully electric aircraft with extremely high energy consumption per passenger will not be viable for large-scale commercial aviation, because energy or hydrogen production still comes at an economic and environmental cost. Fig. 18b demonstrates that the energy per passenger of the FC regional aircraft for the present 300nmi mission will reach the level of the conventional 50-passenger aircraft if the technology advancement is on or above the curve:

- TMS: 3 [kW/kg], Motor: 3.5 [kW/kg], FC: 1.2 [kW/kg]
- TMS: 2.1 [kW/kg], Motor: 7 [kW/kg], FC: 1.75 [kW/kg]
- TMS: 1.7 [kW/kg], Motor: 13 [kW/kg], FC: 3 [kW/kg]

In future work, the mission performance results of different configurations and component designs with different efficiency maps will be placed on Fig. 18b based on the trade-off between weight and energy consumption, both using current and future projected technology factors.

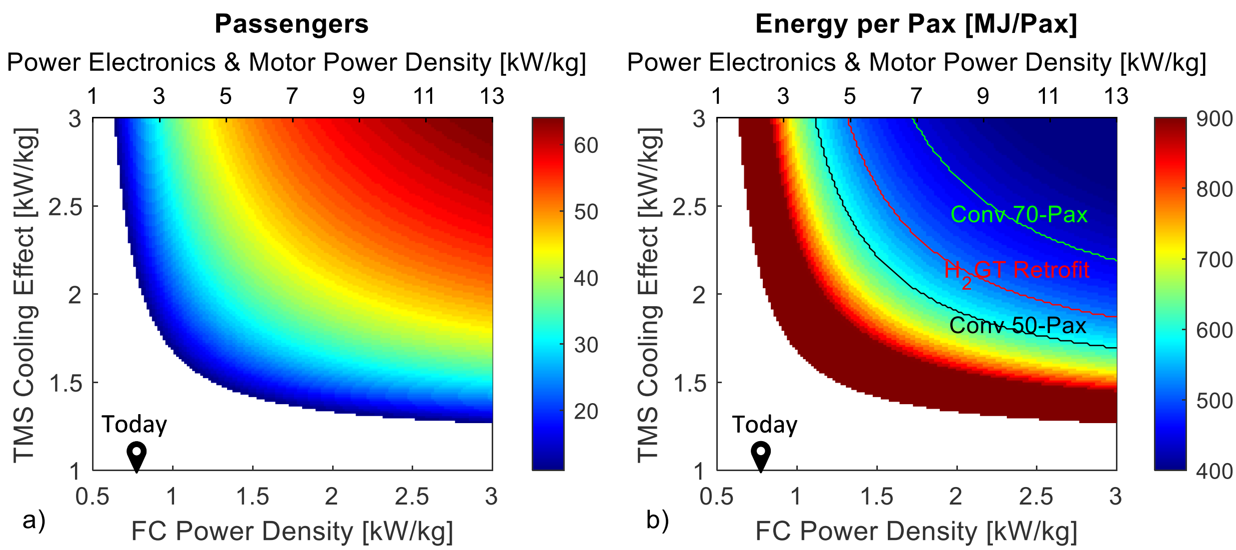

Fig. 18 Number of passengers and energy per passenger for 300nmi and MTOW over a range of TMS, FC, motor and power electronics power density

L. From mission level to electric power system level

The calculations for the electric system power management and distribution are performed at each step of the flight mission. The motor, inverter and converter performance are based on component maps that have been designed for this architecture and power requirement with E-HEART. The fuel cell system exhibits the highest variation in efficiency during the mission, ranging between 50% and 65% based on the power setting and altitude, which affects both the energy/fuel consumption and the heat generation.

The effect of the power requirement, propeller speed and altitude over the flight mission on the electric system performance is demonstrated in Fig. 19. From taxi to cruise, as the altitude increases (Fig. 19e) the difference between the fuel cell stack efficiency and fuel cell system efficiency (Fig. 19b) increases because the compressor power increases to provide the required operating pressure of the fuel cell at higher altitude. For this motor design, the motor efficiency drops at the phases with lower shaft power (Fig. 19a) and shaft speed requirements (Fig. 19c) i.e., taxi and descent. At the phases with lower power requirements (taxi, descent and then cruise), it is observed that the fuel cell output voltage increases, the current decreases and the stack efficiency increases. This behaviour is derived by solving the fundamental equations of the fuel cell model. Finally, it should be noted that the current and voltage of the FC refers to one side of the aircraft (output of the 4 parallel, 4 in series FC configuration).

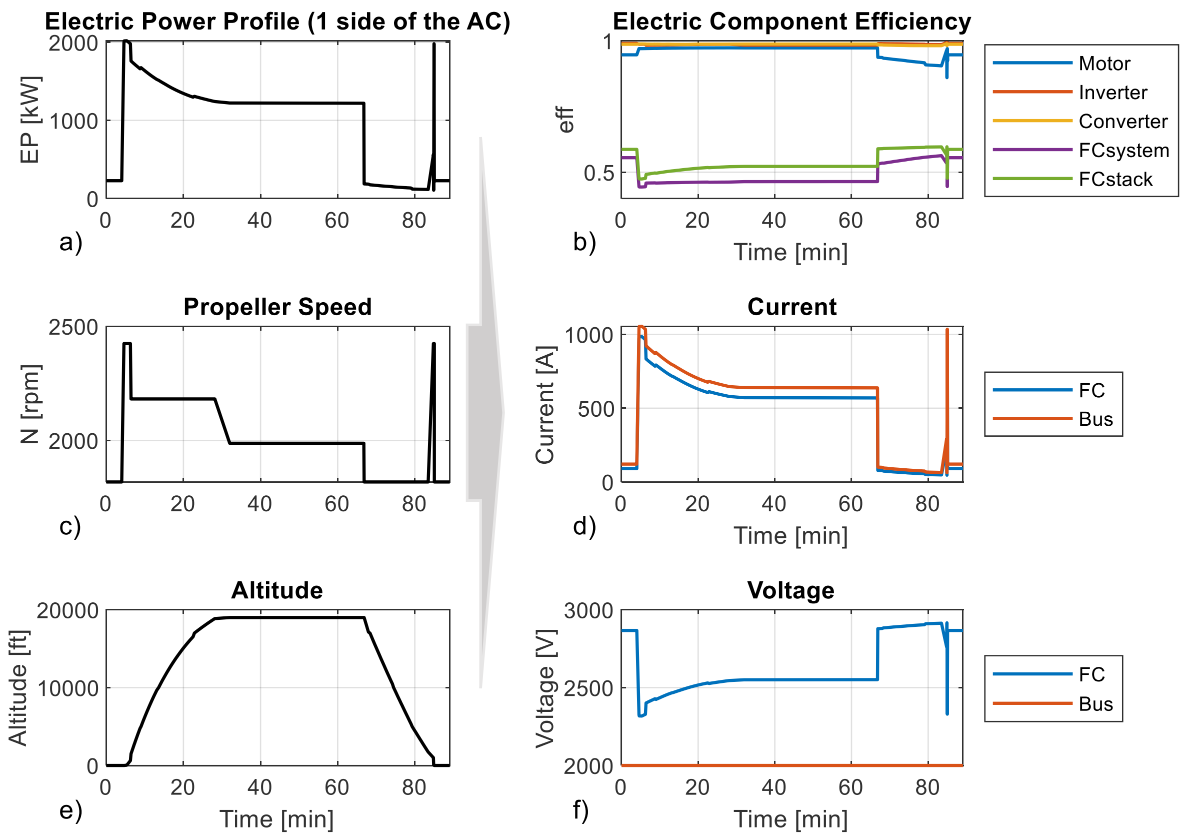

Fig. 19 Effect of mission parameters on electric power system performance

M. From lower fidelity methods to higher fidelity methods

Fig. 20 demonstrates the deviation between a lower fidelity modeling approach that cannot capture the dynamic behavior of the electric power system, and the higher fidelity integrated approach presented in this paper. The deviation of 8.23% in fuel/energy consumption could potentially be ignored in conceptual aircraft design level, however, a more detailed propulsion system design and off-design performance analysis are required to mature new technologies. As will be shown in Section H, table 2, this deviation can be different for different flight conditions and missions.

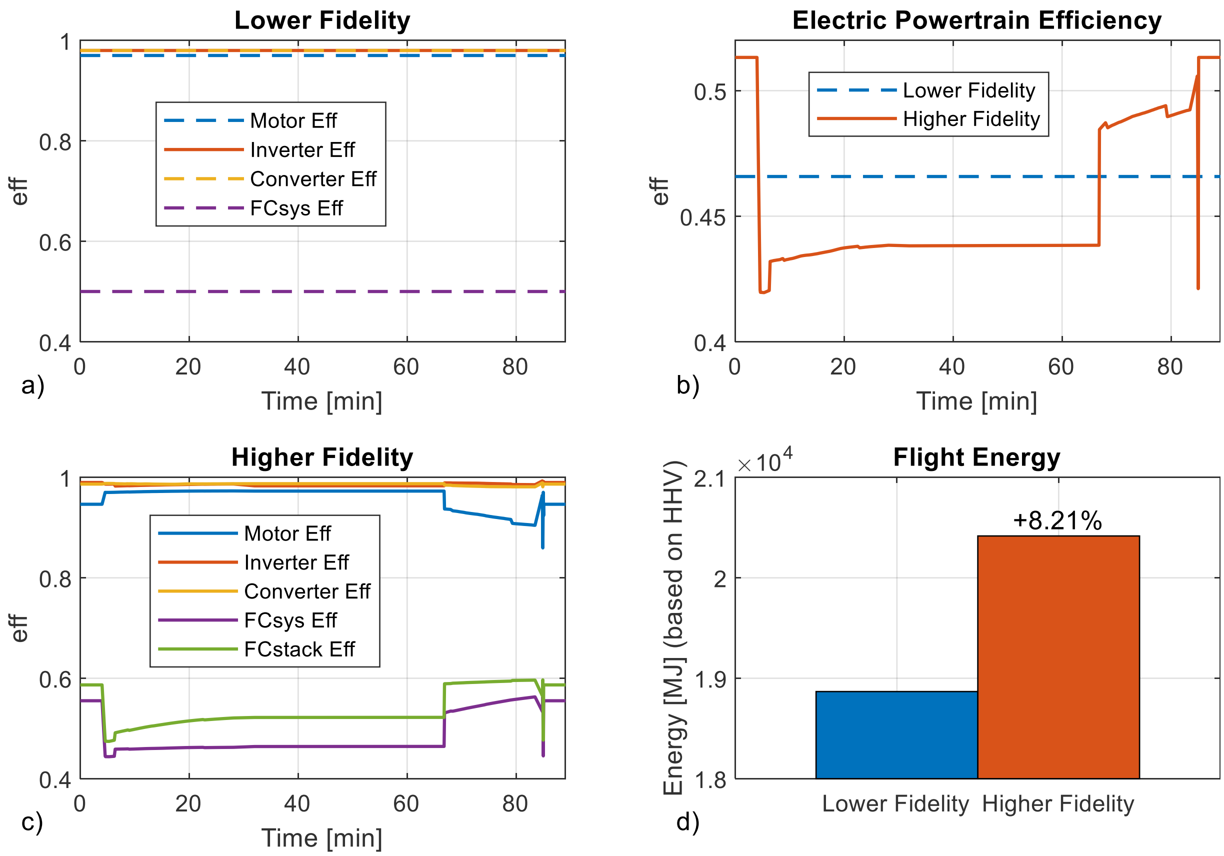

Fig. 20 Deviation between lower fidelity and higher fidelity modelling

N. System performance and interactions under different mission requirements and scenarios

The FC and electric power system are used in various mission requirements and conditions. The reference mission is a 300nmi with MTOW, 0ft take-off altitude, 19000ft cruise altitude, 0.44 cruise Mach and standard conditions. Based on this reference mission, various scenarios are applied such as considering the second leg of an island-hopping mission (reduced payload due to passenger drop-off and fuel burn during the first leg) where the first leg is the reference missions, a 500nmi mission, 2000ft lower cruise altitude, a deviation from ISA standard conditions (dT_{ISA}) of +25K and a combination of $dT_{ISA=}$+25K and take-off from an airport with 2000ft elevation. The flight profile and aircraft weight of the mission scenarios are presented in Fig. 21.

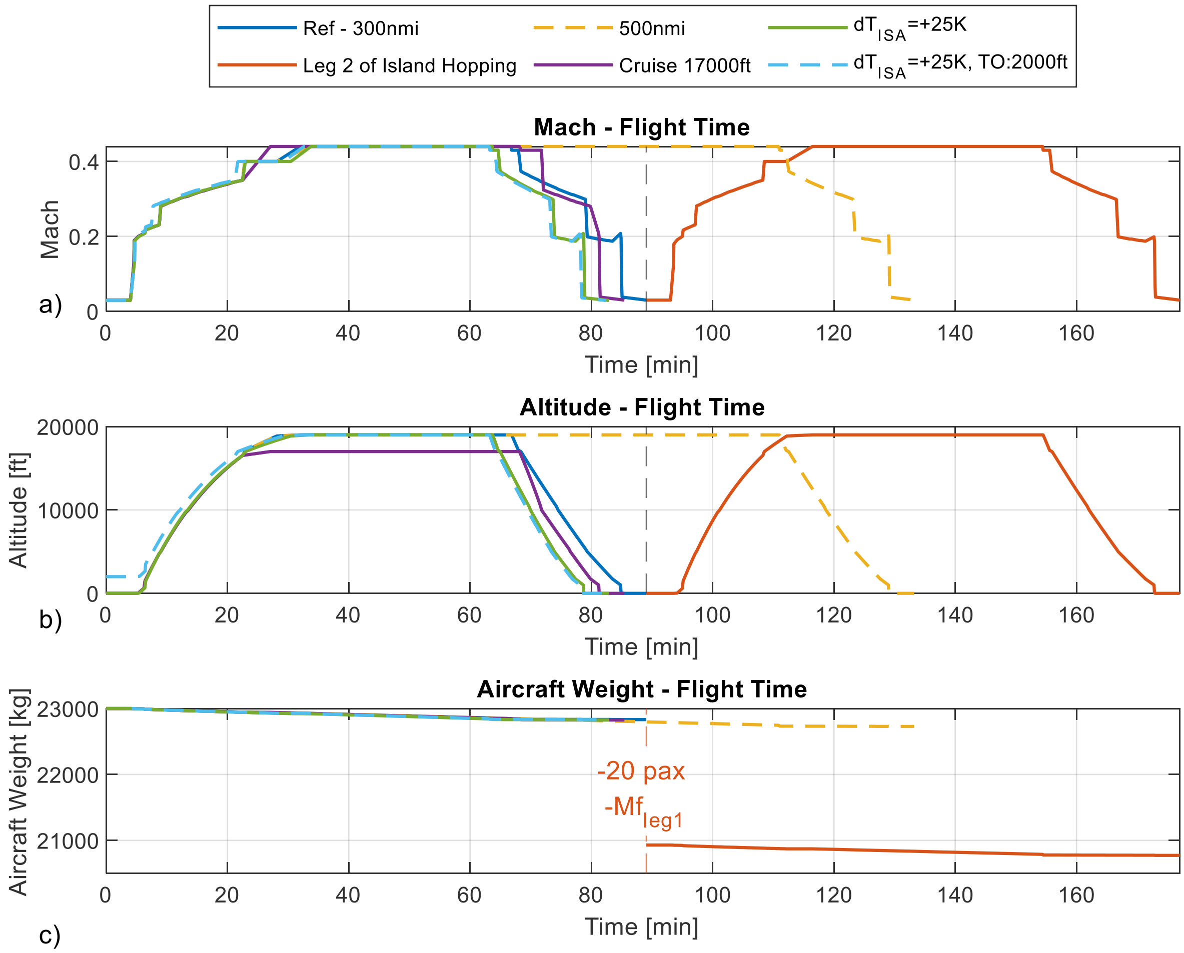

Fig. 21 Flight profile of mission scenarios performed with the FC aircraft retrofit

Various mission scenarios are performed with the same component designs to test if the electric components and FC meet the requirements within the operating limits, and assess the overall system and component performance:

- A reference mission which is the same as in Fig. 11 - Fig. 20 (300nmi, MTOW, cruise at 19000ft and 0.44 Mach and ISA conditions) and against which all the scenarios are compared
- The second leg of an island hopping mission with reduced passengers and with the reference mission being the first leg
- A 500nmi mission
- A mission with 19000ft
- A mission with a +25K temperature deviation from ISA conditions
- A mission with +25K temperature deviation from ISA condition and a take-off altitude of 2000ft

The specifications are the same as the reference mission and only the reported parameters are varied.

The first objective is to identify if the electric component designs and sizing of the FC configuration cover sufficiently the requirements of all the missions and conditions. The maximum operating point of each 600kW PEMFC four in parallel configuration is 550V and 300A, so assuming an equal condition for the FC stacks, the maximum operating point of the FC configuration is 2200V and 1200A. In Fig. 22, it is shown that at the take-off with dT_{ISA}=+25K and 2000ft altitude, the voltage (Fig. 22a) and current (Fig. 22b) of the fuel cell approach the maximum operating the most. There is still a safety margin to account for the effect of degradation and more severe conditions that have not been tested yet, however, a wider design space exploration in the future could push the operating points and conditions closer to the operating limit.

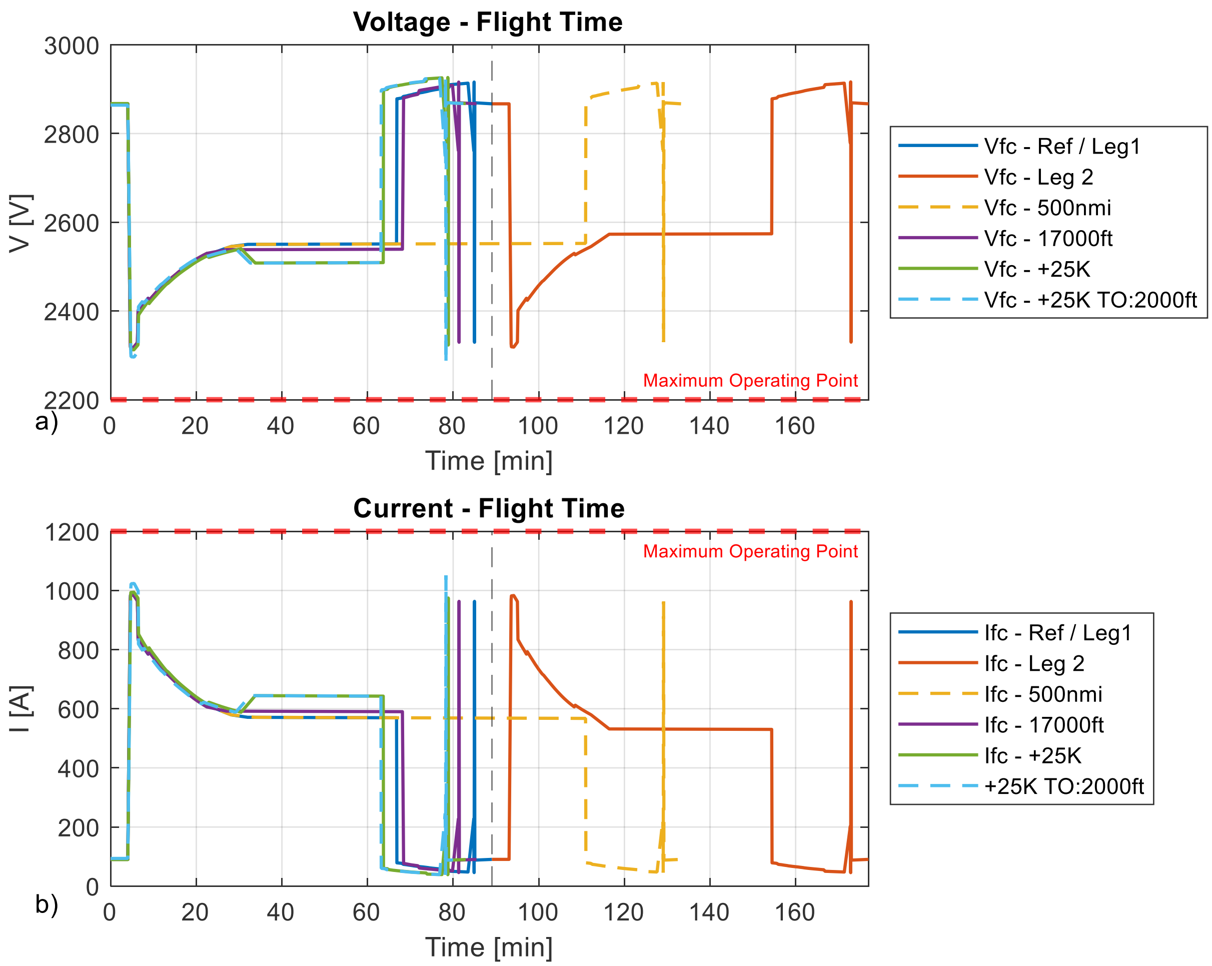

Fig. 22 FC voltage and current against the maximum operating point under various mission scenarios

The operating points of each mission are plotted on the motor map, the inverter map and the converter map. Out of the three electric power components, the motor is the one with the lowest efficiency. At take-off, climb and cruise, which are the most energy-consuming phases due to the higher power, the operating points are on the motor peak efficiency island (Fig. 23a) with only a marginal 0.5% reduction at the take-off hot condition with 2000ft elevation. To ensure that the points are in the peak efficiency regions to improve energy consumption and avoid overheating, the motor was oversized to ensure that the energy-consuming mission points fall within the peak efficiency region of the map. Overall, the peak efficiency region of the motor map offers good coverage of the torque and speed range over the missions. Motor design should be able to manipulate the design so that the mission points fall on the highest efficiency regions of the map. However, at the same time, the impact on motor size should be assessed. Metrics like energy consumption per passenger or kg of payload can capture the trade-off between energy efficiency and system mass.

It should be noted that, with today's technology, the investigated motor design (Fig. 23a), despite being very efficient over the mission, it would come at a great expense of additional mass. The power density for this motor is estimated at around 2 kW/kg today and the motor was sized for a 700kW power limit, so the mass would be around 350kg/motor, and 2800kg for the eight motors. On the other side, if the motor power was designed with a power limit very close to the rated power of the propulsion system (~500kW), around 800kg or total mass could have been saved but at take-off, there would be a risk of overheating and constraints should be imposed regarding the continuous operating time at this power. A motor design trade-off study between efficiency across the mission and motor mass is included in [28]. Further work should investigate the design trade-off between motor efficiency (related to motor power limit), motor mass and operational constraints, and how the optimum trade-off may shift toward choosing higher motor power limit as the technology advances and higher motor power densities are achieved.

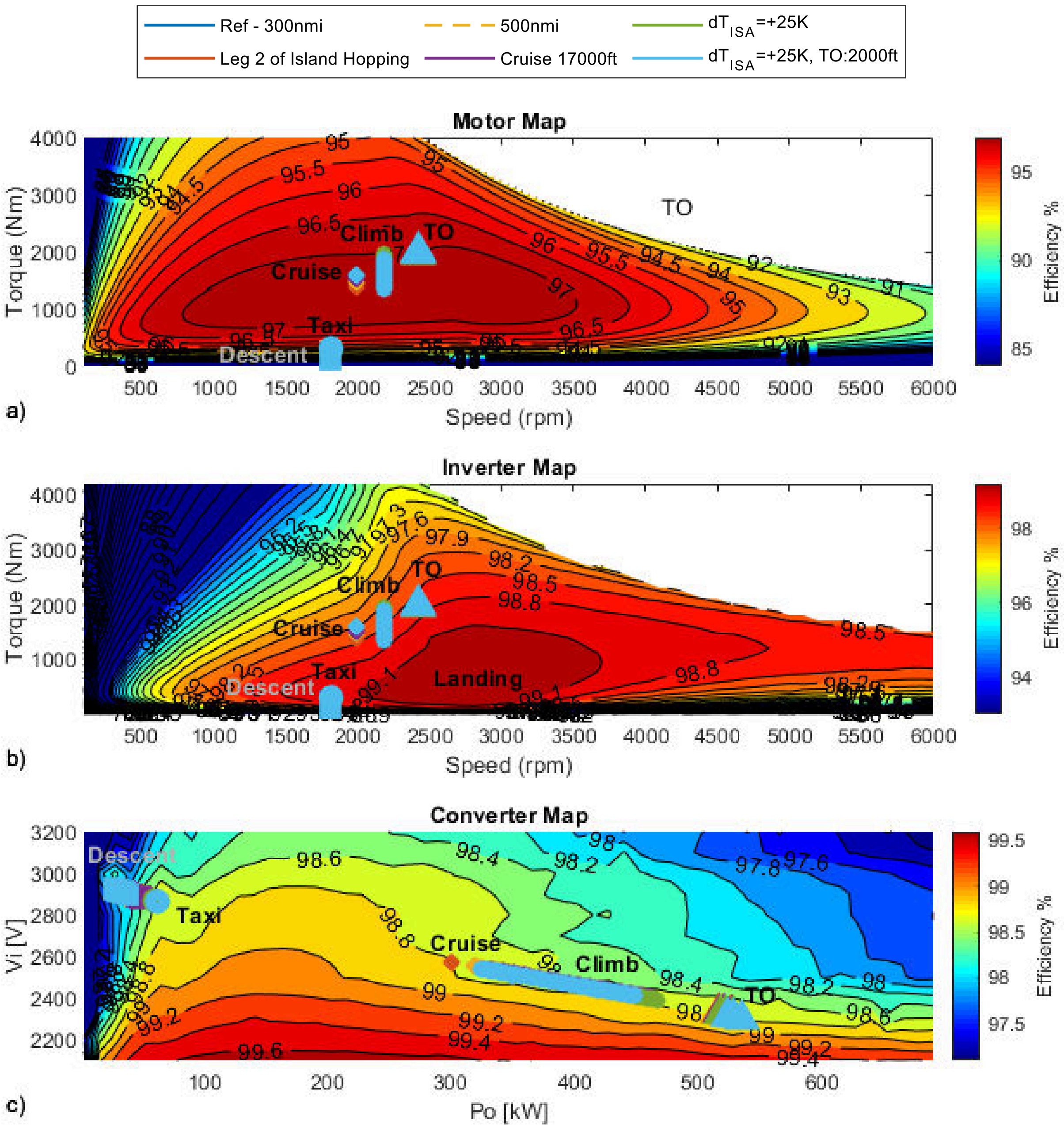

Fig. 23 Operating points on component maps for various mission conditions

In the island hopping scenario, the performance of the propulsion system is calculated in two consecutive missions with passenger drop-off at the end of the first leg. The first leg begins with MTOW (Fig. 21c). The second leg has the same range and cruise altitude but is performed with lighter aircraft weight because of the fuel burn during the first leg and the lower number of passengers (payload). For this reason, the climb is slightly faster, and the thrust requirement is lower during cruise, leading to lower fuel consumption during the second leg. It is also observed that the second leg becomes more efficient. The FC stack efficiency (Fig. 24c) as well as the FC system efficiency (Fig. 24d) are improved at the second leg cruise compared to the first leg cruise. Since the power requirement is lower at the cruise of the second leg, the power required by the compressor is also lower because less fuel and air are provided to the FC, while being at the same cruise altitude (Fig. 21b) and ambient conditions.

When comparing a 500nmi mission against a 300nmi, both missions are initiated with MTOW but as the 500nmi mission continues the cruise for longer, the aircraft weight is reduced for the remainder of cruise (Fig. 21c) which leads to slightly lower fuel consumption and improved FC stack (Fig. 24c) and system efficiency (Fig. 24d). However, the gradient of the aircraft weight change is lower than the conventional aircraft so reduced benefits can be harvested by a long cruise compared to a conventional aircraft (Fig. 11a). The longer-range mission (500nmi) spends a higher percentage of the total time at cruise conditions and a lower percentage at taxi and descent conditions compared to the 300nmi mission. As shown in Fig. 19Fig. 19, the FC efficiency is lower at higher power settings (take-off, climb and then cruise) and higher at the lower power settings (taxi and descent). Consequently, as will be summarized in Table 2, the time-averaged powertrain efficiency becomes lower for the 500nmi mission which has a longer cruise. This is in contrast with the behavior of conventional gas turbine engines which are most efficient at cruise. In conventional gas turbines, the benefit at cruise conditions further increases for longer ranges as the aircraft weight reduces with the fuel burn. However, this benefit is very limited in the FC aircraft because the fuel consumption is 4-5 times lower so the aircraft weight gradient is less aggressive than the conventional aircraft.

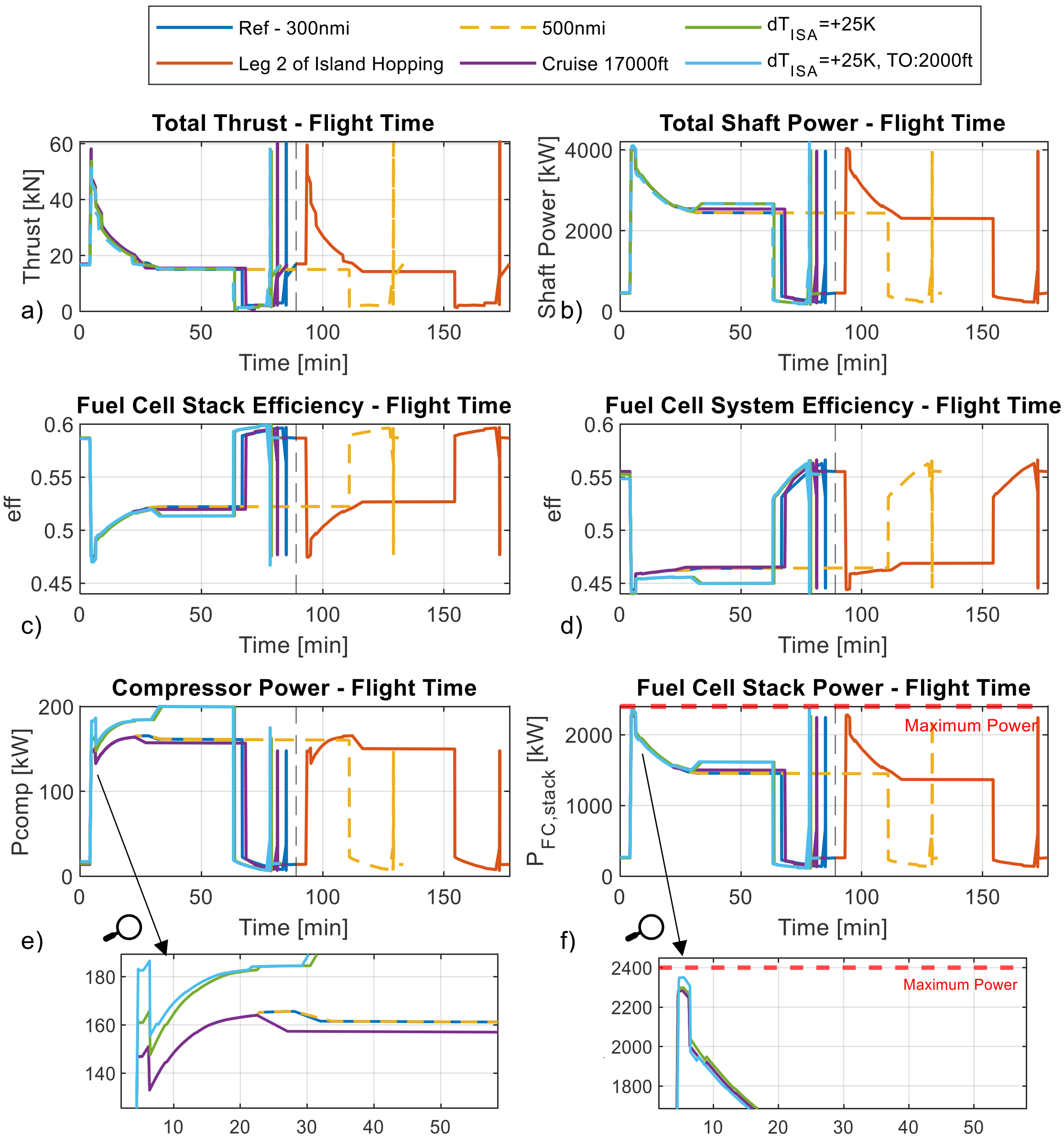

Fig. 24 a) Total aircraft thrust, b) Total aircraft shaft power, c) FC stack efficiency, d) FC system efficiency, e) Compressor power, f) FC stack output power for one FC configuration (four parallel, then four in series) under different mission scenarios

At 17000ft cruise altitude, this aircraft has lower L/D than at 19000ft, and the drag increases due to the higher air density. This results in a 0.5kN higher thrust requirement (Fig. 24a) and about 90kW higher shaft power requirement (Fig. 24b). On one side, at the lower cruise altitude the shaft power requirement of the propeller increases (Fig. 24b) but on the other side, the compressor power requirement reduces (Fig. 24e) because of the higher ambient pressure at lower altitude. Overall, it is concluded that the higher shaft power requirement at 17000ft overcompensates for the fact that less power is extracted by the compressor to provide the necessary air pressure as the net FC power (before the extraction of auxiliary power) is higher at 17000ft than 19000ft (Fig. 24f), which is directly linked with fuel consumption. The fuel cell stack efficiency is 51.9% at 17000ft (Fig. 24c) and 52.2% at 19000ft. However, due to the higher compressor power extraction, the FC system efficiency deviates more from the FC stack efficiency at 19000ft than at 17000ft, so the FC system efficiency curves nearly coincide in Fig. 24b, with the efficiency at 19000ft being only 0.1% lower. The observed trade-off between compressor power requirement and propeller shaft power requirement at different cruise altitudes can be the motivation for a wider design space exploration to investigate if an optimum trade-off between compressor power and shaft power requirement can be identified at some altitude level for each aircraft weight.

The same 300nmi mission is also performed under standard conditions and hot day conditions, which correspond to +0K and +25K temperature deviation from the International Standard Atmosphere (ISA) conditions, respectively. The power setting in terms of output shaft power is kept the same at take-off and climb. For a fixed shaft power (rated power) the propeller delivers lower thrust at take-off and climb due to the lower air density (Fig. 24a), and as a result, the take-off and climb time have increased. The cruise Mach was kept constant (Fig. 21a), but at the hotter conditions, the aircraft velocity at cruise is higher because of the higher speed of sound. The lower air density under hotter conditions tends to reduce the drag of the aircraft, but the increase in aircraft velocity at cruise compensates for that, and eventually, the thrust requirement was calculated nearly the same (Fig. 24a). However, the shaft power requirement of the propeller to maintain the same thrust is higher (Fig. 24b) due to the lower air density. In addition, the fuel cell net power output has increased for the hotter cruise, because of the combination of higher propeller power requirement and increased compessor power requirement (Fig. 24e). Overall the compressor power requirement and fuel cell net power output is increased across the whole mission for the hotter conditions compared to the reference mission.

Finally, the mission with hot conditions at dT_{ISA}=+25K is repeated and the take-off altitude is increased to 2000ft to capture operation in an airport with elevation. In Fig. 24e, the compressor power requirement has further increased from the mission with +25K and take-off altitude at sea level, because of the lower power density at 2000ft take-off altitude. The rated output shaft power of system is still provided to the propeller but the thrust has further reduced

From a pure performance perspective and as long as a suitable TMS system is in place, it can be concluded that the fuel cell stack in isolation is less affected by the change in ambient conditions compared to the gas turbines. The ambient conditions and cruise altitudes indirectly influence the operating point and performance of the FC stack through the variation of the auxiliary power (compressor power and TMS power extraction if VCS is used) which will need to be covered by the FC so the net power output requirement of the FC stacks and their efficiency change. The remainder power at the output of the FC system (including the balance of plant) is transferred through the electric power system to provide the required shaft power to the propeller. The auxiliary system is responsible for providing the necessary operating conditions to the FC but at the same time it is the one that can push the operating point of the FC closer to its operating limit as it was shown in Fig. 22 and Fig. 24e. Depending on how oversized or marginally sized the FC configuration is for the propeller power requirement, operational constraints like a power derate at take-off and aircraft performance deterioration may need to be accepted when the auxiliary power system under demanding ambient conditions pushes the FC operating point towards its limit. Consequently, a need arises to increase the focus and fidelity on the design and modeling of the auxiliary systems.

4. Inputs for TMS design and performance analysis

Modeling the component behavior and the efficiency under different ambient temperatures becomes particularly critical because it will provide the component heat losses to size the TMS and then test its off-design performance. It is observed that the FC efficiency and overall powertrain efficiency drop at hotter ambient temperatures so the additional heat losses at hot conditions should be taken into consideration. In future work, outputs of this modelling framework (Fig. 25) will be used to inform a detailed TMS design and then test it under various operating conditions and missions.

In Fig. 25a, it is demonstrated that the heat losses of the fuel cell at hot take-off conditions increase by 27.9kW. A design choice is available here: The TMS can be oversized for extremely hot conditions (ex. +25K) so the aircraft will carry an extra weight penalty at most missions, or it can be sized for less hot conditions (ex. +15K). In that case, a FC power constraint should be introduced at higher temperatures than +15K in the form of a power derate so that the resulting FC heat losses do not exceed the TMS capability. This is similar to the concept of gas turbine rated power/thrust which can be achieved up to the flat rating temperature. Above that temperature, the rated power/thrust cannot be achieved within the component material limits, so a decrease in the power is applied.

In this context, the new framework will be used to quantify the trade-off between oversizing the TMS and accepting a higher weight penalty and reduced payload capability, and sizing the TMS at less extreme conditions and imposing power and performance constraints at the most extreme conditions.

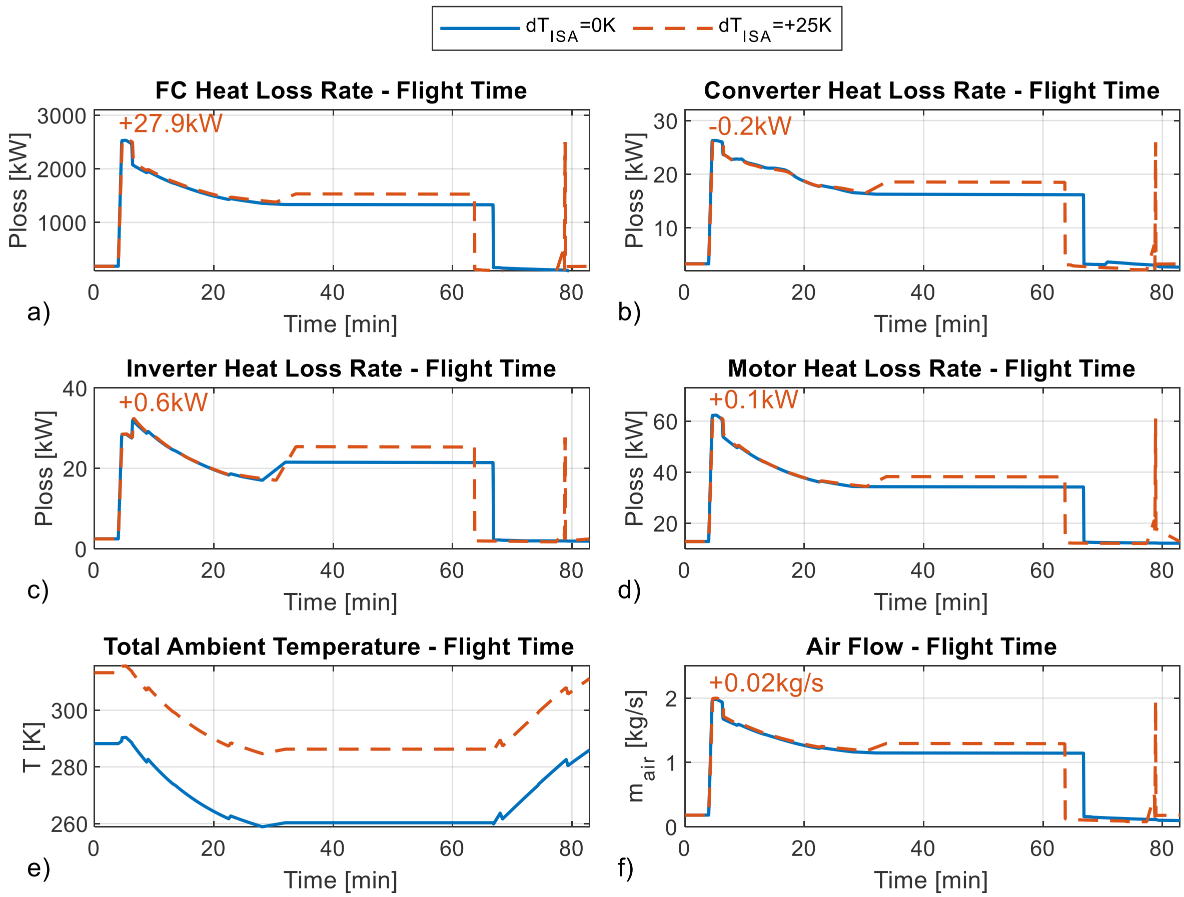

Fig. 25 Heat loss rate during missions with different ambient conditions

5. Evaluation at aircraft level

In Table 2, the consumed hydrogen, the time-averaged powertrain efficiency under different mission scenarios and the take-off performance are summarized and compared against a reference mission. Based on the take-off distances reported for regional aircraft with MTOW = 23000kg, it is considered that the TO performance requirement is <1400m as regional aircraft often operate at smaller airports with shorter runways. If the FC aircraft is operated at airports with longer runways, the payload may not need to be reduced. However, if the TO performance required should be achieved due to smaller airport constraints, a reduction of the payload is suggested.

Table 2 Summary of mission effect on electric propulsion system performance

	Fuel	Average Powertrain Efficiency	TO Length
Reference Mission: 300nmi, MTOW	***170kg***	***45.42%***	***1393m***
Island Hopping (Leg 2, -20pax)	-7.35%	+0.39%	1163m
500nmi	+60.94%	-0.51%	1393m
-2000ft Cruise Altitude	+3.14%	-0.1%	1393m
dT_{ISA} = +25K	+1.6%	-1.08%	1609m
dT_{ISA} = +25K, TO @ 2000ft	+0.41%	-1.11%	1765m

V. Conclusion

An integrated, higher-fidelity platform for modeling and evaluating the flight mission performance of novel propulsion systems was presented. Electric component maps, calculations for the power management and distribution of the electric power system, aircraft and mission performance analysis, gas turbine performance simulation and variable pitch propeller performance maps are integrated within this methodology to capture system interactions.

The mission performance was evaluated both at aircraft level and component level to understand the characteristics of the hydrogen-electric (PEMFC) regional aircraft compared to the conventional aircraft and a hydrogen gas turbine retrofit as a comparison with another emerging hydrogen technology. The propulsion system mass is higher for a FC aircraft retrofit, but the FC aircraft emissions are lower and the overall propulsion efficiency is higher than the hydrogen gas turbine due to the lower fuel consumption by the FC.

Then, the effect of variable mission requirements on the FC propulsion system performance was discussed and the individual components were assessed under various off-design mission conditions to capture the change in efficiency, energy consumption and ensure that all components operate within their limits.

A. Overall Design and Performance Considerations

- The fuel cell propulsion system is more efficient at low power settings while the gas turbine is more efficient at high power settings. This can be the motivation for optimized energy management strategies that use the fuel cell and gas turbines where they are most efficient while satisfying the power requirement.
- For the same mission and MTOW, the fuel cell aircraft has lower fuel consumption during take-off and climb, so it is always heavier than the conventional during climb and ToC. Consequently, for a FC aircraft retrofit, the power requirement increases to achieve the same aircraft performance with the same aircraft platform. Apart from the higher weight, the propeller-driven propulsion system has lost the contribution of the gas turbine residual thrust. As a result, the propellers needs to operate at further increased power to provide additional thrust to compensate both for the loss of gas turbine exhaust thrust and for the heavier ToC.
- In future work, a hybrid propulsion system will be designed by sizing the FC configuration at cruise, where it is more efficient than take-off and climb, and combining it with other energy sources ex. GT and/or batteries to meet take-off and climb requirements. A FC system is heavier when designed for higher power but can operate for longer with small weight penalty (only added fuel), while battery mas has a more significant increase for higher energy capacity (longer duration). At cruise, the power requirement is lower so the FC and electric power system weight as well as TMS requirements can be reduced. However, cruise is a phase with a lot of potential variability so the maximum FC net power should be selected carefully so that it is able to provide the necessary power for any cruise condition, ambient conditions, auxiliary power requirement and drop of efficiency in the rest of the electric power system. Based on the observations from the considered missions, the maximum FC net power for cruise conditions was found to be 1616 kW per side of the aircraft (3232kW for the whole aircraft) and will be used as a first power estimate to resize the FC at cruise.
- Especially for aerospace applications that have highly varying conditions, the FC auxiliary system behavior under variable mission conditions becomes critical, because it can drive the FC operating point towards its limits, resulting in either a need for aircraft operational and performance constraints when a threshold of ambient conditions is reached or resizing the system to account for higher system power requirement. This emerges as a potential design trade-off study which can be further explored in future studies.

B. Sub-System and Component Design and Performance Considerations

- The outputs of this platform will be used as boundary conditions in a detailed TMS design and performance analysis at off-design conditions. The hot day mission or the hot day mission with 2000ft take-off altitude can be selected as the extreme conditions to perform a detailed TMS system design. However, if the sizing conditions for TMS are selected at the most extreme conditions, the TMS will be oversized for the standard, more frequent conditions. However, a design trade-off study between TMS weight and operational constraints is possible using the integrated mission analysis platform. Different TMS sizing conditions that are not the most extreme will be used and then the off-design performance of the system will be tested at extreme conditions. In order not to exceed the temperature limit of the FC, a power constraint can be identified and be recommended as a derate under high temperatures when the design choice is not to oversize the TMS for the most extreme conditions, similar to the gas turbine flat rating temperature concept.
- Electric components, a PEM FC configuration using existing FC stacks and an electric power system were designed and tested under varying mission requirements and conditions to ensure they are within the efficient region and safe operating limits. Similar to the discussion on TMS design considerations, electric components

and FC configurations can be oversized with a huge safety factor to meet any off-design requirement and auxiliary power extraction at the expense of increased OEW and reduced payload capability which in turn increases the energy consumption per passenger. In the present demonstration, oversized motors (700kW power limit) and stack configuration (600kW stack output power) are used to allow a safety factor to cover any power requirement and allow the mission points to be in the highest efficiency regions of the motor map and avoid motor overheating at any condition. A motor design power close to the maximum required of the mission would have reduced the operating empty weight of the aircraft but on the other side it would increase the energy consumption, as the efficiency islands would have shrinked, and motor cooling requirement or the motor could be overheated at take-off. In that case, limits in the maximum continuous operating time under the highest power may need to be introduced. This can be the topic of a comparative study between oversized systems that improve operability and performance in a wide range of condition and reduced system designs that reduce system mass but decrease energy efficiency and impose operational constraints at less extreme conditions.

- The presented mission scenarios, and other scenarios, will be repeated using different component designs from [17] and [28] to compare and identify which design offers the lowest energy consumption and most beneficial weight/efficiency trade-off across a wide range of mission requirements and conditions while operating within safe limits.
- In the uncertainty analysis of the technology factors, it was demonstrated that the passenger capability and flight energy per passenger are highly affected by the technology factors and were compared against the energy per pax of the conventional 50-pax, 70-pax and hydrogen GT retrofit. The combinations of minimum power densities were indentified for the FC regional aircraft to reach the energy per passenger of today's conventional aircraft. Further to the trade-off studies suggested above, different design choices may become beneficial when moving from lower power densities to higher power densities based on the progress of the enabling technologies. Until the component power densities and TMS technology reach higher levels, it may be beneficial to avoid oversizing the system to reduce the OEW of the aircraft but sacrifice aircraft performance at demanding conditions by imposing operating constraints, while in an optimistic scenario for future power densities, oversizing the system to improve operability, reliability and energy efficiency may become the best design practice due to the reduced weight penalty. A wider design exploration will further explore this trade-off in future work.

References

[1] *Destination 2050-A Route to Net Zero European Aviation Preface*.

[2] Kazula, S. *Review of Fuel Cell Technologies and Evaluation of Their Potential and Challenges for Electrified Propulsion Systems in Commercial Aviation*.

[3] Palladino, V., Jordan, A., Bartoli, N., Schmollgruber, P., Pommier-Budinger, V., and Benard, E. Preliminary Studies of a Regional Aircraft with Hydrogen-Based Hybrid Propulsion. 2021.

[4] Pastra, C. L., Cinar, G., and Mavris, D. N. Feasibility and Benefit Assessments of Hybrid Hydrogen Fuel Cell and Battery Configurations on a Regional Turboprop Aircraft. 2022.

[5] Wroblewski, G. E., and Ansell, P. J. Mission Analysis and Emissions for Conventional and Hybrid-Electric Regional Jet Aircraft. 2018.

[6] Orefice, F., Nicolosi, F., Corcione, S., Vecchia, P. della, Ciliberti, D., and Ruocco, M. Hybridization and Mission Analysis of a Regional Turboprop. 2021.

[7] Liu, Y., Wang, H., Zhang, J., Jiang, T., and Zheng, Y. Retrofit and New Design of Regional Aircraft with Hybrid Electric Propulsion. 2021.

[8] Cinar, G., Cai, Y., Bendarkar, M. v., Burrell, A. I., Denney, R. K., Mavris, D. N., and Shielding, M. System Analysis and Design Space Exploration of Regional Aircraft with Electrified Powertrains. 2022.

[9] Marksel, M., and Prapotnik Brdnik, A. "Maximum Take-Off Mass Estimation of a 19-Seat Fuel Cell Aircraft Consuming Liquid Hydrogen." *Sustainability (Switzerland)*, Vol. 14, No. 14, 2022. https://doi.org/10.3390/su14148392.

[10] ZeroAvia. ZeroAvia Conducts UK's First Commercial-Scale Electric Flight. ZeroAvia Conducts UK's First Commercial-Scale Electric Flight. Accessed Dec. 1, 2022.

[11] H2FLY. H2FLY Vision. https://www.h2fly.de/vision. Accessed Dec. 1, 2022.

[12] Future Flight. ENGINE MAKER MTU TEAMS WITH DLR ON HYDROGEN FUEL CELL PROPULSION PROJECT. https://www.futureflight.aero/news-article/2020-08-13/engine-maker-mtu-teams-dlr-hydrogen-fuel-cell-propulsion-project. Accessed Dec. 2, 2022.

[13] Laskaridis, P., Valencia, E., Kirner, R., and Wei, T. J. Assessment of Distributed Propulsion Systems Used with Different Aircraft Configurations. 2015.

[14] Sanders, D. S., and Laskaridis, P. "Full-Aircraft Energy-Based Force Decomposition Applied to Boundary-Layer Ingestion." *AIAA Journal*, Vol. 58, No. 10, 2020, pp. 4357–4373. https://doi.org/10.2514/1.J058695.

[15] Kirner, R., Raffaelli, L., Rolt, A., Laskaridis, P., Doulgeris, G., and Singh, R. "An Assessment of Distributed Propulsion: Advanced Propulsion System Architectures for Conventional Aircraft Configurations." *Aerospace Science and Technology*, Vol. 46, 2015, pp. 42–50. https://doi.org/10.1016/j.ast.2015.06.022.

[16] Zhou, T., Enalou, H. B., Pontika, E., Zaghari, B., and Laskaridis, P. Minimising the Effect of Degradation of Fuel Cell Stacks on an Integrated Propulsion Architecture for an Electrified Aircraft. 2022.

[17] Zaghari, B., Zhou, T., Enalou Balaghi, H., Pontika, E., Kipouros, T., and Laskaridis, P. "The Impact of Multi-Stack Fuel Cell Configurations on Electrical Architecture for a Zero Emission Regional Aircraft." *AIAA SciTech Forum*, 2023.

[18] Hanumanthan, H., Stitt, A., Laskaridis, P., and Singh, R. "Severity Estimation and Effect of Operational Parameters for Civil Aircraft Jet Engines." *Proceedings of the Institution of Mechanical Engineers, Part G: Journal of Aerospace Engineering*, Vol. 226, No. 12, 2012, pp. 1544–1561. https://doi.org/10.1177/0954410011424854.

[19] Abu, A. O., Eshati, S., Laskaridis, P., and Singh, R. "Aero-Engine Turbine Blade Life Assessment Using the Neu/Sehitoglu Damage Model." *International Journal of Fatigue*, Vol. 61, 2014, pp. 160–169. https://doi.org/10.1016/j.ijfatigue.2013.11.015.

[20] Laskaridis, P., Pilidis, P., and Kotsiopoulos, P. An Integrated Engine-Aircraft Performance Platform for Assessing New Technologies in Aeronautics. 2005.

[21] ATR. *ATR72-600 Factsheet*.

[22] European Aviation Safety Agency (EASA). *Type-Certificate Data Sheet for Engine PW100 Series*. 2013.

[23] Hosking, E., Kenny, D. P., McCormick, R. I., Moustapha, S. H., Sampath, P., and Smailyes, A. A. The PW100 Engine: 20 Years of Gas Turbine Technology Evolution. 1998.

[24] Drela, M. QMIL/QPROP. https://web.mit.edu/drela/Public/web/qprop/.

[25] Drela, M. *QPROP Formulation*. Cambridge, Massachusetts, USA, 2006.

[26] Filippone, A. *Advanced Aircraft Flight Performance*. 2010.

[27] Janikovic, J. "Gas Turbine Transient Performance Modeling for Engine Flight Path Cycle Analysis." Vol. U617280, 2010.

[28] Kiran, A., Zaghari, B., Sinnige, T., Pontika, E., Enalou, B. H., Kipouros, T., and Laskaridis, P. "The Impact of Electric Machine and Propeller Coupling Design on Electrified Aircraft Noise and Performance." *AIAA SciTech Forum 2023*, 2023.

[29] Shah, S., Rashid, A., and Bhatti, M. *Direct Quadrate (D-Q) Modeling of 3-Phase Induction Motor Using MatLab / Simulink*. 2012.

[30] Recalde, A., Bozhko, S., Atkin, J., and Sumsurroah, S. Optimal Voltage for More Electric Aircraft Direct Current Cabling System. 2021.

[31] Vratny, P. C., Kuhn, H., and Hornung, M. "Influences of Voltage Variations on Electric Power Architectures for Hybrid Electric Aircraft." *CEAS Aeronautical Journal*, Vol. 8, No. 1, 2017, pp. 31–43. https://doi.org/10.1007/s13272-016-0218-z.

[32] Souleman, N. M., Tremblay, O., and Dessaint, L. A. "A Generic Fuel Cell Model for the Simulation of Fuel Cell Power Systems." *2009 IEEE Power and Energy Society General Meeting, PES '09*, 2009, pp. 1722–1729. https://doi.org/10.1109/PES.2009.5275853.

[33] Zhou, T., Enalou Balaghi, H., Pontika, E., Zaghari, B., and Laskaridis, P. Minimising the Effect of Degradation of Fuel Cell Stacks on an Integrated Propulsion Architecture for an Electrified Aircraft. 2022.

[34] Kellermann, H., Fuhrmann, S., Shamiyeh, M., and Hornung, M. "Design of a Battery Cooling System for Hybrid Electric Aircraft." *AIAA Aviation and Aeronautics Forum and Exposition, AIAA AVIATION Forum 2021*, 2021, pp. 1–16. https://doi.org/10.2514/6.2021-3138.

[35] Affonso, W., Tavares, RenataT., Barbosa, F. R., Gandolfi, R., dos Reis, R. J. N., da Silva, C. R. I., Kipouros, T., Laskaridis, P., Enalou, H. B., Chekin, A., Kukovinets, A., Gubernatorov, K., Ravikovich, Y., Ivanov, N., Ponyaev, L., and Holobtsev, D. "System Architectures for Thermal Management of Hybrid-Electric Aircraft - FutPrInt50." *IOP Conference Series: Materials Science and Engineering*, Vol. 1226, No. 1, 2022, p. 012062. https://doi.org/10.1088/1757-899x/1226/1/012062.

[36] Black, A., Crossley, W., and van Seeters, P. Investigations of Perspectives for Re-Engining Commercial Single-Aisle Transport Aircraft. 2012.

[37] Gao, Y., Jausseme, C., Huang, Z., and Yang, T. "Hydrogen-Powered Aircraft: Hydrogen-Electric Hybrid Propulsion for Aviation." *IEEE Electrification Magazine*, Vol. 10, No. 2, 2022, pp. 17–26. https://doi.org/10.1109/MELE.2022.3165725.

[38] Aerospace Technology Institute. *Fuel Cells Roadmap Report - FlyZero*. 2022.

[39] McKinsey & Company. "Hydrogen-Powered Aviation: A Fact-Based Study of Hydrogen Technology, Economics, and Climate Impact by 2050." No. May, 2020. https://doi.org/10.2843/471510.

[40] Huete, J., Nalianda, D., and Pilidis, P. "Impact of Tank Gravimetric Efficiency on Propulsion System Integration for a First-Generation Hydrogen Civil Airliner." *Aeronautical Journal*, Vol. 126, No. 1302, 2022, pp. 1324–1332. https://doi.org/10.1017/aer.2022.60.

[41] Byahut, S., and Uranga, A. Propulsion Powertrain Component Modeling for an All-Electric Aircraft Mission. 2020.

[42] Chandrasekaran, N., and Guha, A. "Study of Prediction Methods for NOx Emission from Turbofan Engines." *Journal of Propulsion and Power*, Vol. 28, No. 1, 2012, pp. 170–180. https://doi.org/10.2514/1.B34245.

[43] ATR. *ATR: The Optimum Choice for a Friendly Environment*. Blagnac Cedex, France, 2001.

[44] ICAO. *ICAO Carbon Emissions Calculator Methodology - Version 10*. 2017.

[45] Voigt, C., Kleine, J., Sauer, D., Moore, R. H., Bräuer, T., le Clercq, P., Kaufmann, S., Scheibe, M., Jurkat-Witschas, T., Aigner, M., Bauder, U., Boose, Y., Borrmann, S., Crosbie, E., Diskin, G. S., DiGangi, J., Hahn, V., Heckl, C., Huber, F., Nowak, J. B., Rapp, M., Rauch, B., Robinson, C., Schripp, T., Shook, M., Winstead, E., Ziemba, L., Schlager, H., and Anderson, B. E. "Cleaner Burning Aviation Fuels Can Reduce Contrail Cloudiness." *Communications Earth and Environment*, Vol. 2, No. 1, 2021. https://doi.org/10.1038/s43247-021-00174-y.